

University of Louisville

ThinkIR: The University of Louisville's Institutional Repository

Electronic Theses and Dissertations

5-2019

Defects in fetal mouth movement and pharyngeal patterning underlie cleft palate caused by retinoid deficiency.

Regina Friedl
University of Louisville

Follow this and additional works at: <https://ir.library.louisville.edu/etd>



Part of the [Animal Structures Commons](#), [Biology Commons](#), [Developmental Biology Commons](#), [Developmental Neuroscience Commons](#), [Disease Modeling Commons](#), [Embryonic Structures Commons](#), and the [Nervous System Commons](#)

Recommended Citation

Friedl, Regina, "Defects in fetal mouth movement and pharyngeal patterning underlie cleft palate caused by retinoid deficiency." (2019). *Electronic Theses and Dissertations*. Paper 3157.
<https://doi.org/10.18297/etd/3157>

This Master's Thesis is brought to you for free and open access by ThinkIR: The University of Louisville's Institutional Repository. It has been accepted for inclusion in Electronic Theses and Dissertations by an authorized administrator of ThinkIR: The University of Louisville's Institutional Repository. This title appears here courtesy of the author, who has retained all other copyrights. For more information, please contact thinkir@louisville.edu.

DEFECTS IN FETAL MOUTH MOVEMENT AND PHARYNGEAL PATTERNING
UNDERLIE CLEFT PALATE CAUSED BY RETINOID DEFICIENCY

By
Regina Friedl
B.S. Biology, Walsh University, 2014

A Thesis
Submitted to the Faculty of the
School of Dentistry at the University of Louisville
In Partial Fulfillment of the Requirements
For the degree of

Master of Science in Oral Biology

Department of Oral Immunology and Infectious Diseases
University of Louisville
Louisville, Kentucky

May 2019

DEFECTS IN FETAL MOUTH MOVEMENT AND PHARYNGEAL PATTERNING
UNDERLIE CLEFT PALATE CAUSED BY RETINOID DEFICIENCY

By

Regina Friedl
B.S. Biology, Walsh University, 2014

Thesis Approved on

April 16th 2019

By the following Thesis Committee:

Dr. Lisa Sandell. Ph. D.

Thesis Director

Dr. Huizhi Wang, Ph.D., M.D.

Committee Member

Dr. Jixiang Ding, Ph.D.

Committee Member

Dr. Juhi Bagaitkar, Ph.D.

Committee Member

DEDICATION

This thesis is dedicated to my parents Greg and Debra Friedl and my sister Anne Marie Friedl who have given me support as well as sacrificed themselves to give me opportunities to pursue my educational goals.

ACKNOWLEDGEMENTS

I would like to thank Swetha Raja for her previous thesis work and significant contributions she put forth that allowed my project to unfold. Without the experiments and data she generated, my project would not have progressed in the way it did.

I want to thank my committee members Dr. Juhi Bagaitkar, Dr. Jixiang Ding, and Dr. Huizhi Wang for their input and support in guiding my thesis to completion. I am truly grateful for their time and suggestions which encouraged me to perfect my work.

I want to extend my appreciation to Dr. Melissa Metzler for offering advice and guidance to navigate my experiments and teaching me lab techniques. Her input guided me in my statistical analysis and data interpretation. Furthermore, her expertise in mouse handling and guidance throughout, helped me to complete my experiments. I am so grateful for each contribution and to be able to work alongside her throughout my research project.

I would like to sincerely thank my mentor, Dr. Lisa Sandell, for giving me the opportunity to join her lab. With no mouse experience, and minimal knowledge in developmental biology, she took a chance on accepting me into her lab. I am so grateful to her for the time she took to teach me and work with me throughout my

time in the Master's Program at University of Louisville. She has given me a greater appreciation for learning and asking probing questions to understand biological processes and mechanisms.

Additionally, I want to thank Dr. Sandell for actively participating in my project throughout, and taking each setback as a learning opportunity, seeking out the answer that our data was telling us. She helped me perfect my research into a publication format, a privilege I know would not have been possible over my time here without her help. It has truly been my pleasure to work under the supervision of such an outstanding mentor and researcher. Dr. Sandell has encouraged me and supported me to fulfill my dreams and educational goals. I feel honored to have been a part of the Sandell Lab during my time at University of Louisville and know that the experience I gained will carry into my next chapter.

ABSTRACT

DEFECTS IN FETAL MOUTH MOVEMENT AND PHARYNGEAL PATTERNING UNDERLIE CLEFT PALATE CAUSED BY RETINOID DEFICIENCY

Regina Friedl

April 16th, 2019

Cleft palate is a common birth defect. Etiologic mechanisms of palate cleft include defects in palate morphogenesis, mandibular growth, or spontaneous fetal mouth movement. Cleft palate linked to deficient fetal mouth movement has been demonstrated directly only in a single experimental model of loss of neurotransmission. Here, using retinoid deficient mouse embryos, we demonstrate directly for the first time that deficient fetal mouth movement and cleft palate occurs as a result of mis-patterned development of pharyngeal peripheral nerves and cartilages. Retinoid deficient embryos were generated by inactivation of retinol dehydrogenase 10 (*Rdh10*), which is critical for production of Retinoic Acid (RA) during embryogenesis. Using X-ray microtomography (microCT), *in utero* ultrasound, *ex vivo* culture, and tissue staining, we demonstrate that retinoid deficient mouse embryos lack fetal mouth movement owing to mis-patterning of pharyngeal cartilages and motor nerves. Findings from this study may indicate the earliest marker for diagnosing cleft palate.

TABLE OF CONTENTS

<u>Acknowledgements:</u>	iv
<u>Abstract:</u>	vi
<u>List of Tables</u>	x
<u>List of Figures</u>	xi
<u>Chapter 1: Introduction and Background</u>	1
<u>1.1 Secondary Palate Formation</u>	1
<u>1.2 Cleft Palate Birth Defects</u>	5
<u>1.3 The Swallowing Apparatus</u>	9
<u>1.4 Vitamin A Metabolism</u>	12
<u>Chapter 2: Materials and Methods</u>	16
<u>2.1 Mouse Strains</u>	16
<u>2.2 Genetic Crosses and Conditional <i>Rdh10</i> Inactivation by Tamoxifen</u> <u>Administration</u>	18
<u>2.3 Nuclear Fluorescent Imaging of Palate Tissues</u>	19
<u>2.4 Histology by Hematoxylin and Eosin Staining</u>	19
<u>2.5 Immunostaining of Paraffin Sectioned and Whole Mount Embryos</u>	20

<u>2.6 Assessment of Palate Fusion in <i>Ex Vivo</i> Cultured Maxillary Explants</u> 21
<u>2.7 MicroCT Analysis of Embryos</u> 22
<u>2.8 X-Gal Staining to Assess RARE-LacZ Reporter Gene Expression</u> 23
<u>2.9 qPCR</u> 24
<u>2.10 Skeletal Stain with Alizarin Red and Alcian Blue</u> 26
<u>2.11 Ultrasound Imaging</u> 27
<u>2.12 Statistical Analysis</u> 27
<u>Chapter 3: Results</u> 29
<u>3.1 Stage Specific Inactivation of <i>Rdh10</i> Induces Secondary Cleft Palate</u> 29
<u>3.2 Culture of Isolated Maxillae <i>Ex Vivo</i> Suggests Extrinsic defect Underlies Retinoid Deficient Cleft Palate</u> 37
<u>3.3 Retinoid Deficient Embryos do not Exhibit Micrognathia</u> 41
<u>3.4 The Tongue of <i>Rdh10</i>^{delta/flox} Mutant Embryos Obstructs Shelf Elevation</u>	.. 45
<u>3.5 <i>Rdh10</i>^{delta/flox} Mutant Embryos have Defects in Motor Nerves of the Posterior Pharyngeal Arches</u> 52
<u>3.6 Retinoid Deficient Embryos Develop Defects in the Pharyngeal Skeleton</u> 56
<u>3.7 Conditional Inactivation of <i>Rdh10</i> Disrupts Pharyngeal Anterior-Posterior Patterning Genes, Consistent with Other RA Deficiency Models</u> 61
<u>3.8 <i>In Utero</i> Spontaneous Mouth Movement is Restricted in <i>Rdh10</i>^{delta/flox} Mutant Embryos</u> 68

<u>Chapter 4: Discussion</u>	76
<u>4.1 Identifying the Role of Retinoic Acid in Palate Development</u>	76
<u>4.2 Novel Identification for Fetal Mouth Immobility</u>	81
<u>4.3 Cleft Palate in <i>Rdh10^{delta/flox}</i> Mutant Embryos is likely caused by a Combination of Defects in Nerve Routing and Muscle Attachment</u>	82
<u>4.4 RA Deficiency Etiology in Cleft Palate Make Have Implications in Other Contexts</u>	85
<u>Chapter 5: Conclusions</u>	87
<u>References</u>	88
<u>Curriculum Vitae</u>	97

LIST OF TABLES

<u>Table 1: <i>Rdh10</i> Mutant Strains and Transgenic Alleles Used in This Study</u>	18
<u>Table 2: Primers used for qPCR Gene Expression Analysis</u>	26
<u>Table 3: Frequencies of Pharyngeal Cartilage Defects.</u>	59

LIST OF FIGURES

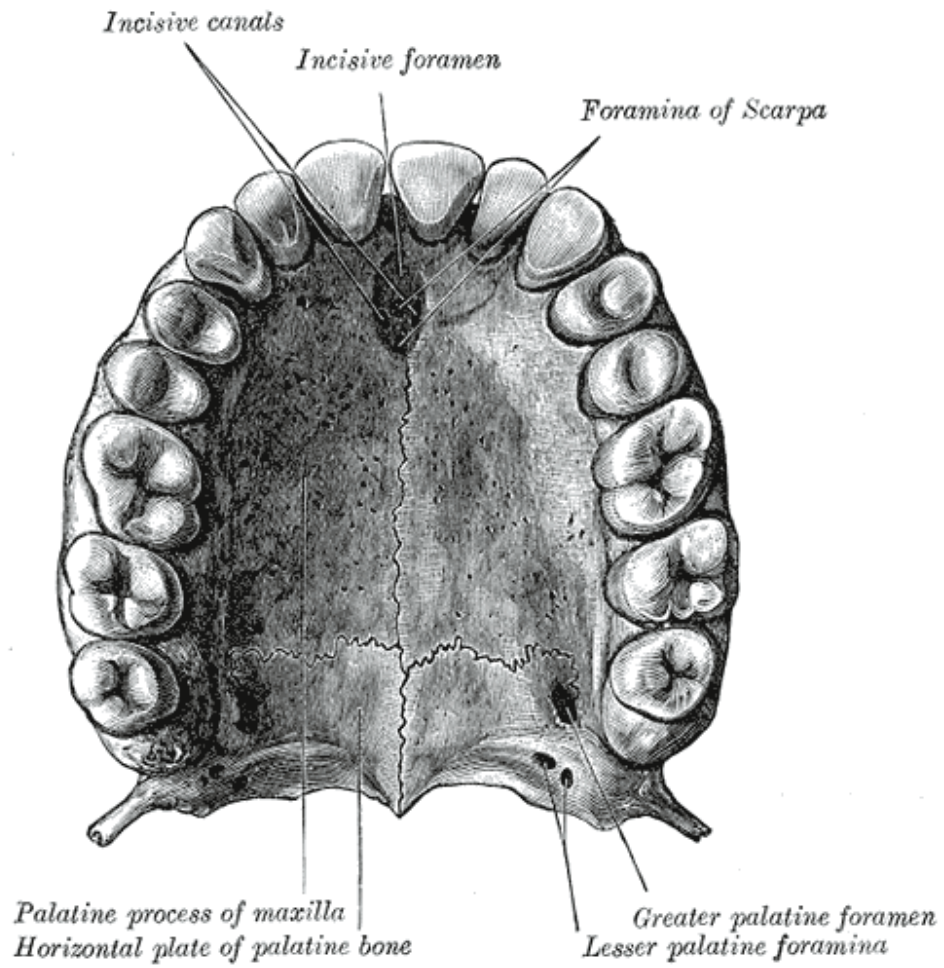
<u>Figure 1.</u> Schematic of the Palate and Palatine Structures	3
<u>Figure 2.</u> Developmental Stages of Secondary Palate Formation in Mouse.....	5
<u>Figure 3.</u> Schematic Representation of Intrinsic vs. Extrinsic to the Palate	9
<u>Figure 4.</u> The Pharyngeal Arches During Development	12
<u>Figure 5.</u> Vitamin A Metabolism.....	14
<u>Figure 6.</u> Morphological Comparison of Control and Mutant Embryos	32
<u>Figure 7.</u> Bone and Cartilage Staining with Alizarin Red and Alcian Blue of E16.5 Embryos.	34
<u>Figure 8.</u> Histological Analysis of Control and <i>Rdh10^{delta/flox}</i> Mutant Embryos	36
<u>Figure 9.</u> Three Day <i>Ex Vivo</i> Culture of Control and Mutant Maxillary Explants..	39
<u>Figure 10.</u> Histological Analysis of Control and <i>Rdh10^{delta/flox}</i> Mutant Embryos after Three-Day Culture	41
<u>Figure 11.</u> Alizarin Red and Alcian Blue Stain for Mandibular Analysis	44
<u>Figure 12.</u> Measurements for Mandibular Size Analysis.....	45
<u>Figure 13.</u> Analysis of Embryo Morphology by MicroCT.	47
<u>Figure 14.</u> Volumetric Analysis of Control and Mutant Tongues	50
<u>Figure 15.</u> Muscle Morphology Analysis of Control and Mutant Embryos.....	52
<u>Figure 16.</u> Schematic of Nerve Staining of an E10.5 Embryo.....	54
<u>Figure 17.</u> Nerve Outgrowth Analysis of CN XII and C1	56

<u>Figure 18.</u> Pharyngeal Skeleton Analysis with Alcian Blue Staining.	58
<u>Figure 19.</u> Muscle Attachment Analysis of Tongue Musculature to the Hyoid Bone	61
<u>Figure 20.</u> RARE LazC Analysis with Whole Mount Specimens and Histology...	63-64
<u>Figure 21.</u> Schematic Representation of the Region that was used for qPCR Analysis	66
<u>Figure 22.</u> Expression of Pharyngeal Anterior-Posterior Patterning Genes	68
<u>Figure 23.</u> Control Ultrasound Still and Movement Schematic	71
<u>Figure 24.</u> Mutant Ultrasound Still and Movement Schematic... ..	73
<u>Figure 25.</u> Statistical Comparison of Ultrasound Movements	75
<u>Figure 26.</u> Schematic Drawing of the Pharyngeal Arch Elements that are Involved in Swallowing.....	79
<u>Figure 27.</u> Schematic Drawing of Proposed Mechanism for the Role of Vitamin A and RA in Palate Formation	81

CHAPTER 1: INTRODUCTION AND BACKGROUND

1.1 Secondary Palate Formation

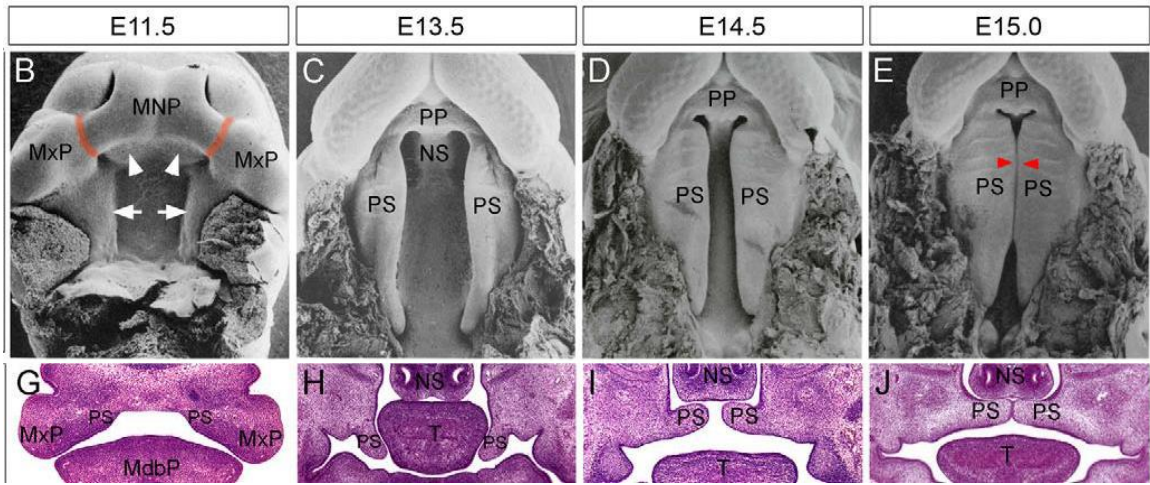
The palate is the physical separation of a bony dome between the nasal cavity and the oral cavity in humans and other mammals. Its function is to facilitate proper movement of food during mastication as well as allow breathing to be uninhibited by food intake. The palate is divided into two different portions; the primary palate, which develops from the fronto-nasal prominence, and the secondary palate, which forms from the maxillary process. The primary palate exists anterior to the incisive foramen, while the secondary palate, which includes the palatine bones and soft palate, exists posterior to the incisive foramen (Fig.1).



From: Gray's Anatomy

Figure 1. Schematic of the Palate and Palatine Structures

In mouse, formation of the secondary palate begins on day embryonic day 12.5 (E12.5) and involves downward growth of the palatal shelves until E13.5. Tissue remodeling, accompanied by horizontal outgrowth from the medial edge of the palate shelves occurs at E14.5, further growth towards the midline happens at E15.5, and finally fusion of the shelves by degradation of the midline epithelial seam is completed at E16.5 (Fig. 2) (Bush & Jiang, 2012; Jin et al., 2010; Sperber, 2002).



Adapted from Bush et al 2012 (used with permission)

Figure 2. Developmental Stages of Secondary Palate Formation in Mouse

Red arrows mark initial site of palate adhesion. MxP= maxillary Process, MNP= medial nasal process, PP= primary palate , PS= palate shelves, NS=nasal septum, T= tongue

The morphogenic events of palate closure are not isolated but occur within the context of overall growth of the orofacial complex. As the palate shelf tissue remodels and grows medially, growth and expansion of the entire facial complex results in downward and forward displacement of the mandible and tongue, opening space above in which the palate shelves elevate. The descent of the mandible/tongue and elevation of the palate shelves occur around 8-12 weeks gestation in humans (Burdi & Faist, 1967; Sperber, 2002; Yoon, Chung, Seol, Park, & Park, 2000), or embryonic day 14.5 (E14.5) in mice (Walker, 1969). Concurrently, the facial muscles become innervated by the motor and sensory nerves, that activate the muscles that move the tongue and mandible. In addition to the morphogenic growth and movement of embryonic facial structures, spontaneous neuromuscular movement of the mandible and tongue begins at this stage (de Vries, Visser, & Prechtel, 1985; Walker, 1969; Wragg, Smith, & Borden, 1972). The spontaneous mouth movements involve a backwards tilt of the head away from the chest, opening of the mandible, and retraction and protrusion of the tongue. These movements coordinate the neuromuscular actions of swallowing amniotic fluid (J. L. Miller, Sonies, & Macedonia, 2003), and prepare the fetus for suckling after birth.

1.2 Cleft Palate Birth Defects

The complexity of the process of palate formation during embryogenesis is reflected in the high incidence of palate clefts. Orofacial clefts are among the most common human structural birth defects. Cleft lip/palate occurs at a prevalence of ~1/1000 live births worldwide (Parker et al., 2010; World Health

Organization, 2007). Such clefts cause harsh physical limitations resulting in suffering to the individual in social aspects as well as imposing a fiscal burden the individual and family (Wehby & Cassell, 2010). Although research has elucidated the cause and helped in prevention of many cleft palate etiologies, many causes of cleft palate that remain unidentified.

In humans, cleft palate can occur independent of other abnormalities, or in the context of a syndrome, associated with a characteristic set of phenotypes. Two syndromes that include cleft palate are Pierre Robin sequence and 22q11.2 deletion syndrome. In patients with Pierre Robin sequence cleft palate occurs as result of micrognathia, a small mandible, which crowds the tongue and obstructs palate shelf elevation during embryogenesis (Giudice et al., 2018). Patients with 22q11.2 deletion syndrome, also known as DiGeorge syndrome, have a spectrum of abnormalities including cleft palate, orofacial malformations, and defects in development of the pharyngeal arch derivatives (LaMantia et al., 2016; McDonald-McGinn et al., 2015). A key phenotype of this syndrome is congenital difficulty in feeding and swallowing, known as dysphagia (LaMantia et al., 2016; C. K. Miller, 2009). Transgenic mice have helped to determine that the mechanism of dysphagia is a hypoglossal neurotransmission defect that impairs swallowing function (Karpinski et al., 2014; Wang, Bryan, LaMantia, & Mendelowitz, 2017).

Known etiologic mechanisms of palate cleft include defects in palate morphogenesis, defects in mandibular growth, and defects in spontaneous fetal mouth movement. Most studies on cleft palate focus primarily on defects within

the palate tissues, which are considered “intrinsic” (palate defects). A smaller cohort of studies have evaluated “extrinsic” palate defects such as defects in mandible size that can also result in cleft palate (Fig. 3).

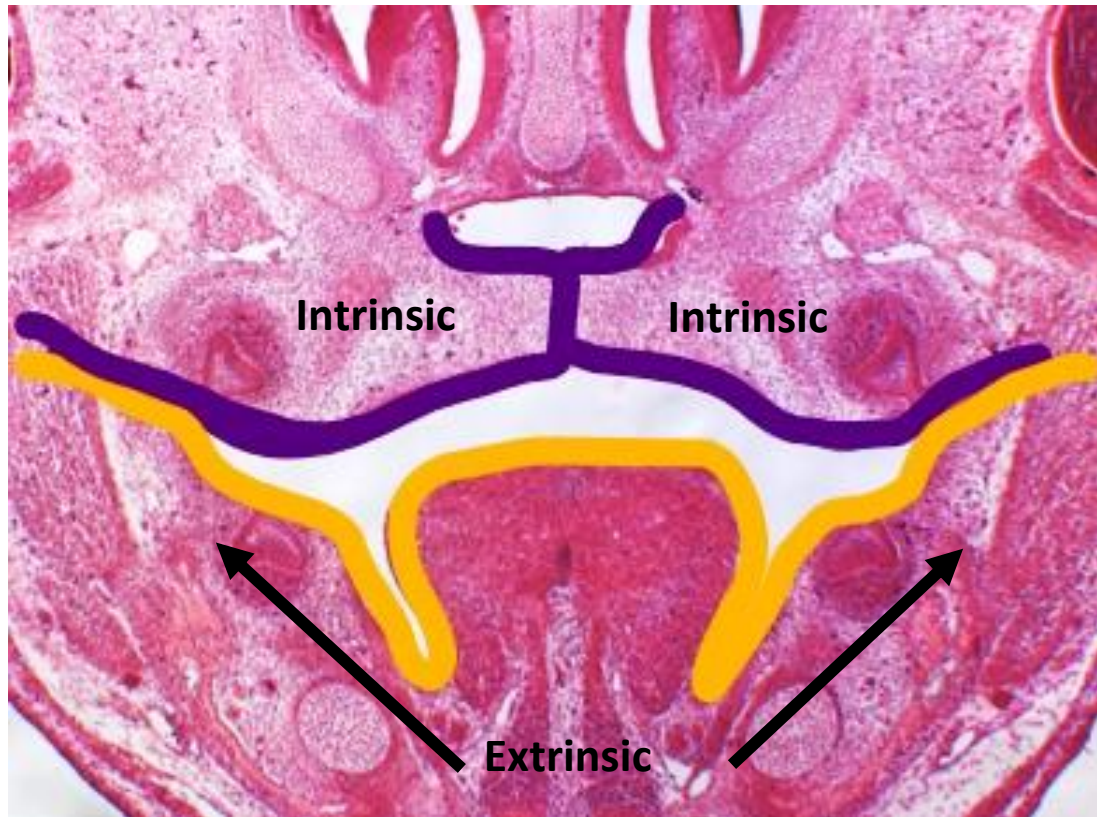


Figure 3. Schematic Representation of Intrinsic vs. Extrinsic to the Palate. If a defect causing cleft palate is intrinsic, it would be caused by something located within the purple region. An extrinsic defect would be in the yellow region or below (not within the purple region which depicts the palate shelf tissues).

Additionally, notable defects have been identified in the development of the extrinsic tongue musculature, likely causing loss of tongue function, which correlates exactly with the prevalence of cleft palate in *Hoxa2* mutant mice (Barrow & Capecchi, 1999). A more recently identified defect in fetal mouth immobility has been directly linked to defective neurotransmission that prevents any movement *in utero* (Asada et al., 1997; Condie, Bain, Gottlieb, & Capecchi, 1997; Culiati et al., 1995; Homanics et al., 1997; Oh, Westmoreland, Summers, & Condie, 2010; Tsunekawa, Arata, & Obata, 2005; Wojcik et al., 2006). The existing studies on fetal mouth movement have inferred that fetal mouth movement is required for palate shelf formation and post-natal development. However, to date, only one experimental study directly demonstrates that cleft palate can result from fetal mouth immobility due to defective neurotransmission. In summary, mechanistic insights into how defects in fetal mouth movement contribute towards cleft palate are incompletely characterized.

1.3 The Swallowing Apparatus

Swallowing and mouth opening are complex processes and are essential to embryonic and neonatal development and post-natal survival. Incorporating movements of mouth opening and tongue withdrawal, these movements require many anatomical elements such as muscles, bones and cartilages, as well as innervation of motor nerves. Many of the muscles that open and close the jaw are attached at the hyoid bone and thyroid and cricoid cartilages. These same skeletal elements are essential to anchor muscles of the tongue. The hypoglossal motor nerve (CN XII) innervates the tongue and controls tongue

withdrawal. Cervical nerve 1(C1) innervates the geniohyoid muscle, and controls movement of hyoid bone during swallowing.

Importantly, the nerves, bone, and cartilages involved in mouth movement and swallowing are derived from the pharyngeal arches during embryonic development (Fig. 4).

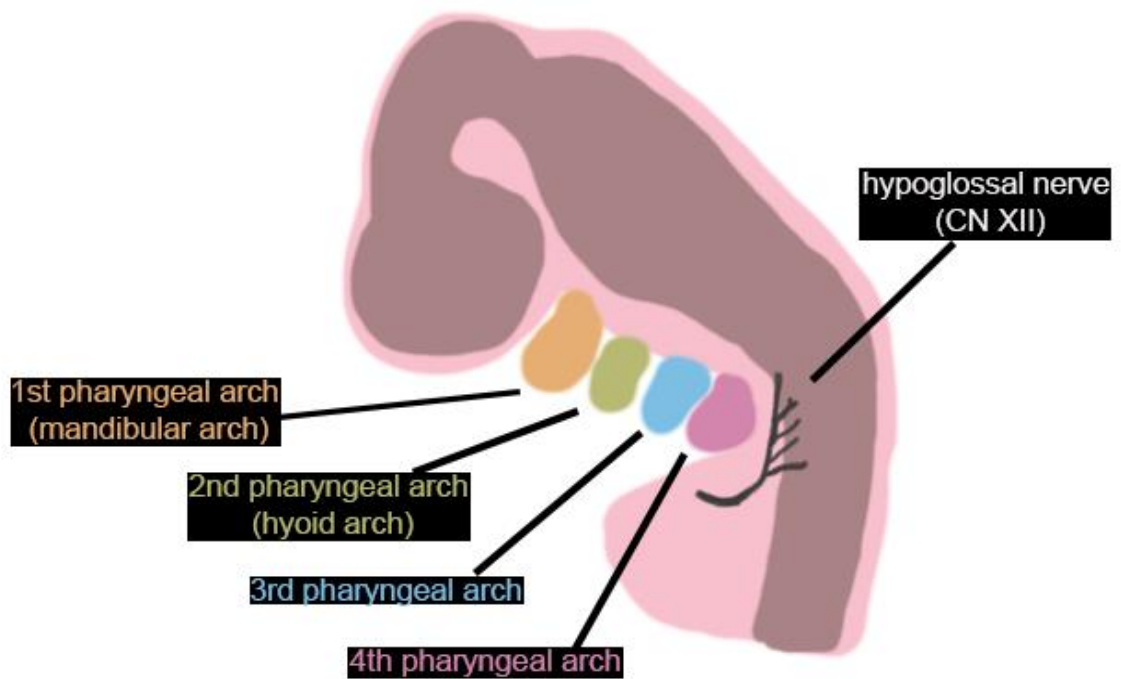


Figure 4. The Pharyngeal Arches During Development. The pharyngeal arches are early development structures that give rise to different anatomical elements of the head and neck. 1st arch gives rise to the maxilla and mandible while the 2nd through 6th arches gives rise to many features of the head and neck. The hypoglossal is the motor nerve that innervates the tongue muscles.

The second through sixth pharyngeal arches develop into fundamental components of the head and neck critical for swallowing. It is well established that development of the pharyngeal arches is orchestrated by retinoid signaling, and that perturbation of retinoid levels results in defects of the pharyngeal arch-derived elements (Mark, Ghyselinck, & Chambon, 2004; Wendling, Dennefeld, Chambon, & Mark, 2000).

1.4 Vitamin A Metabolism

Retinoic acid (RA) is the active metabolite of the dietary small molecule Vitamin A. Collectively Vitamin A and its derivatives are known as retinoids. The metabolic conversion of Vitamin A to RA is accomplished via two sequential oxidative reactions, the first of which is mediated in mouse embryos primarily by the enzyme RDH10 (Fig. 5) (Duester, 2008; K. Niederreither & Dolle, 2008; L. L. Sandell, Lynn, Inman, McDowell, & Trainor, 2012; L. L. Sandell et al., 2007).

Vitamin A is metabolized into the active component RA

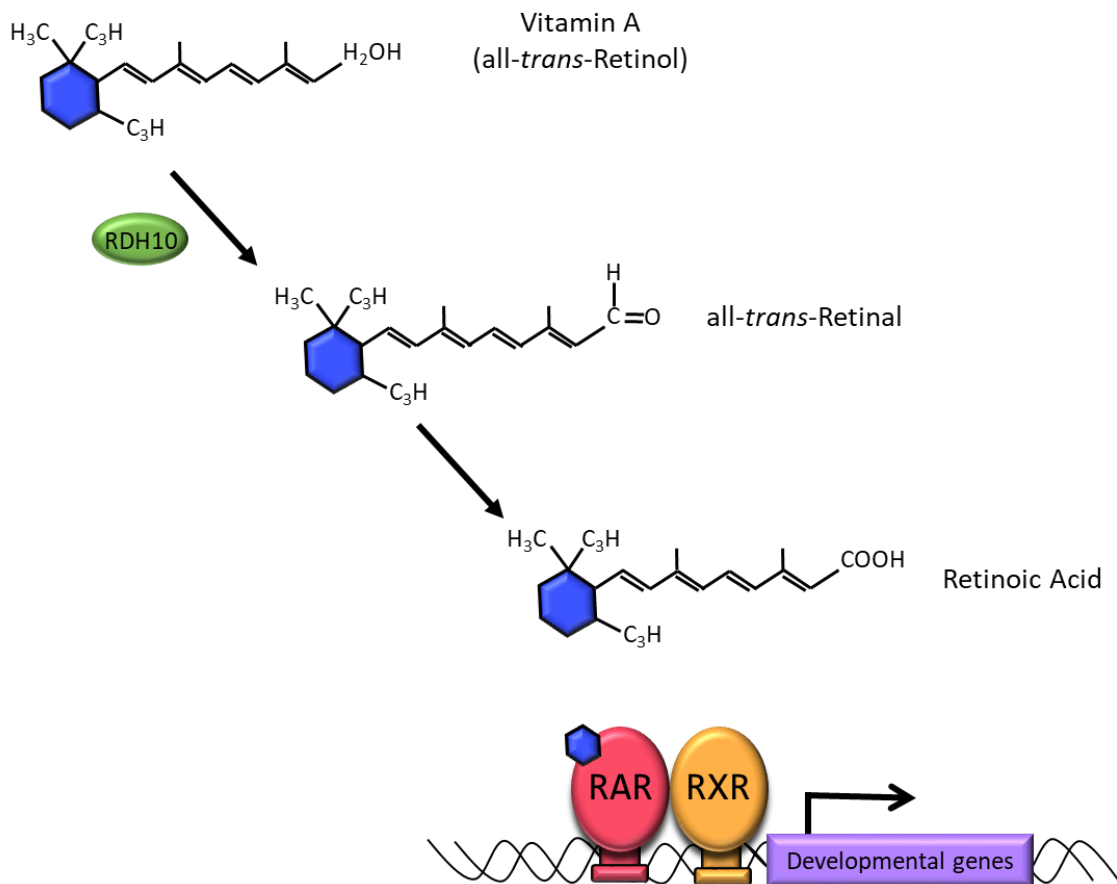


Figure 5. Vitamin A Metabolism. This is a schematic representation of the Vitamin A metabolic pathway. Vitamin A or retinol is converted into its active form, RA, via two oxidation reactions. The first reaction is a critical regulatory step in this pathway and is mediated by the enzyme RDH10 which converts retinol into the intermediate metabolite, retinaldehyde (*all-trans*-retinal).

RA is an important signaling molecule that regulates many aspects of adult health and embryonic development. One developmental role of RA that has been extensively studied is the regulation of embryonic anterior-posterior patterning, which occurs largely via transcriptional regulation of *Hox* gene family members (Aida Halilagic et al., 2007; A. Halilagic, Zile, & Studer, 2003; Hernandez, Putzke, Myers, Margaretha, & Moens, 2007; Rhinn & Dolle, 2012; Ribes, Wang, Dolle, & Niederreither, 2006; Schneider, Hu, Rubenstein, Maden, & Helms, 2001; Sirbu, Gresh, Barra, & Duester, 2005).

Homeostatic levels of RA must be tightly controlled within embryonic tissues, as excess or insufficiency both disrupt embryogenesis (Cunningham & Duester, 2015; Metzler & Sandell, 2016; K. Niederreither & Dolle, 2008). RA is a well-known teratogen (Hand, 2012; McCaffery, Adams, Maden, & Rosa-Molinar, 2003; Piersma, Hessel, & Staal, 2017). Malformations resulting from RA perturbation include defects in pharyngeal arch derived tissues (Mark et al., 2004; Wendling et al., 2000) and cleft palate (Hale, 1935; Aida Halilagic et al., 2007; Lohnes et al., 1994; L. L. Sandell et al., 2007; Josef Warkany, 1945; J. Warkany, Nelson, & Schraffenberger, 1943; Wilson, Roth, & Warkany, 1953; Zhang et al., 2014). There are many proposed mechanisms for cleft palate occurrence under RA excess, some of which offer conflicting insights, leaving room for further investigation on this topic (Hu, Gao, Liao, Tang, & Lu, 2013; Huang, Lu, Chen, & Liao, 2003; Nelson, Levi, & Longaker, 2011; Okano, Suzuki, & Shiota, 2007; Okano, Udagawa, & Shiota, 2014).

Cleft palate resulting from RA excess has been well documented (Hu et al., 2013; Huang et al., 2003; Nelson et al., 2011; Okano et al., 2007). However, the developmental mechanisms of palate formation that are disrupted when RA is insufficient are still unknown. Despite the lack of understanding the developmental mechanisms of palate formation due to insufficient RA signaling, many studies have shown that deprivation of Vitamin A, and therefore reduced RA, will produce cleft palate (Hale, 1935; Josef Warkany, 1945; J. Warkany et al., 1943; Wilson et al., 1953). Because RA production is regulated by enzymatic reactions, we can manipulate this pathway in order to elucidate the endogenous role of RA in palate development and possible new mechanisms causing cleft palate. Here we use conditional *Rdh10* transgenic mice to investigate the link between pharyngeal neuro-skeletal morphogenesis, fetal mouth movement, and palate formation.

CHAPTER 2: MATERIALS AND METHODS

2.1 Mouse Strains

All experiments within this study that involved mice were performed in accordance to the protocol that was approved by the institutional animal care and use committee (IACUC) at the University of Louisville. The approval number for the same is #18727. All mouse strains used are listed with official names in Table 1. The *Rdh10* mutant strains used in this study have been previously described (L. L. Sandell et al., 2012). All mutant *Rdh10* alleles derived from *Rdh10*^{Bgeo/+} ES cells were obtained from the trans-NIH Knockout Mouse Project (KOMP) Repository, a NCCR-NIH supported strain repository (www.komp.org; email service@komp.org). For the experiments described in this study the *Rdh10*^{flox/flox}, and *Rdh10*^{delta/+} mice were bred extensively to FVB/NJ such that their background is mixed with significant contribution of FVB/NJ. Additional mouse strains used were FVB/NJ, RARE-LacZ, and Cre-ERT2, all obtained from Jackson Laboratories and maintained at the University of Louisville. Genotyping of all *Rdh10* alleles and transgenes, from tissue samples of embryos and adult breeder animals, was performed by the commercial genotyping service Transnetyx using primer sequences described by Sandell et al, 2012 (L. L. Sandell et al., 2012).

Table 1. *Rdh10* Mutant Strains and Transgenic Alleles used in this Study

Strain	Background	Reference
<i>Rdh10^{flox/flox}</i>	mixed (primarily FVB/NJ)	(L. L. Sandell et al., 2012)
<i>Rdh10^{delta/+}</i>	mixed (primarily FVB/NJ)	(L. L. Sandell et al., 2012)
Cre-ERT2 <i>Gt(ROSA)26Sor^{tm1(cre/ERT2)Tyj}</i>	mixed	(Ventura et al., 2007)
RARE-LacZ Tg(RARE-Hspa1b/LacZ)12Jrt	mixed	(Rossant, Zirngibl, Cado, Shago, & Giguere, 1991)

2.2 Genetic Crosses and Conditional *Rdh10* Inactivation by Tamoxifen

Administration

In order to obtain embryos at specific developmental stages, we set timed matings. The appearance of a vaginal plug was considered embryonic day 0.5. The *Rdh10* alleles used in this study include *Rdh10*⁺, which denotes the wild type allele, *Rdh10*^{delta}, which denotes a targeted knockout null allele with exon2 deleted, and *Rdh10*^{flox}, a floxed allele in which exon2 is excised upon exposure to Cre recombinase, thereby converting to *Rdh10*^{delta} (L. L. Sandell et al., 2012). With the exception of the ultrasound analysis, we used the following genetic cross for all experiments in this study to produce control and mutant embryos. Homozygous *Rdh10*^{flox/flox}; Cre ERT2/Cre ERT2 mice were paired with *Rdh10*^{delta/+} mice. In litters resulting from these crosses 50% of embryos were *Rdh10*^{flox/+} “control” embryos that were heterozygous for the haplosufficient wild type allele of *Rdh10*, and 50% of embryos were *Rdh10*^{delta/flox} “mutant”, heterozygous for a deleted allele and a conditional floxed allele of *Rdh10*. In these crosses all embryos had a single copy of Cre-ERT2. For the ultrasound experiment, the crosses performed included *Rdh10*^{flox/flox} Cre ERT2/Cre ERT2 mated with *Rdh10*^{flox/flox}, yielding litters in which 100% of embryos were *Rdh10*^{flox/flox} “mutant” with a single copy of Cre-ERT2. For the ultrasound experiments control embryos were obtained by crossing *Rdh10*^{+/+} by *Rdh10*^{+/+}, yielding litters in which 100% of embryos were *Rdh10*^{+/+} “control”. For all time mated animals, a single dose of tamoxifen was administered at E8.5 via maternal oral gavage to activate Cre recombinase and delete *Rdh10* exon 2

in embryos carrying the *Rdh10^{flox}* allele. Each pregnant dam was administered an oral gavage dose of 5 mg of tamoxifen + 2 mg progesterone in 250 μ l of corn oil. Tamoxifen was prepared as follows: 20 mg/ml of Tamoxifen (Sigma-Aldrich-#T5648), was dissolved first at a concentration of 500 μ g/ μ l in absolute ethanol and subsequently diluted to a final concentration of 20 mg/ml in Corn Oil (VWR-#700000-136). The solution was vortexed every 30 minutes and incubated at 55°C until crystals were dissolved (~3-4 hours). Once tamoxifen was dissolved, progesterone (Sigma Aldrich-# P3972) was added to a final concentration 8 mg/ml, and the mixture was incubated at 55°C, with vortexing every 15 minutes until progesterone dissolved (~30 minutes). The solution was then aliquoted into single dose tubes and stored at -20°C for up to two weeks.

2.3 Nuclear Fluorescent Imaging of Palate Tissues.

Morphology of whole mount palates and maxillary explants were imaged by nuclear fluorescent staining and fluorescent stereomicroscopy (Lisa L. Sandell, Kurosaka, & Trainor, 2012). Whole mount specimens were fixed in 4% paraformaldehyde overnight, rinsed in PBS, and stained in DAPI dilactate to final working dilution concentration of 10 nM in PBS solution at room temp, with gentle rocking overnight. DAPI stained specimens were then imaged using a UV light source on a Leica stereomicroscope.

2.4 Histology by Hematoxylin and Eosin Staining

For paraffin sectioning and histology, embryos were harvested and fixed overnight in 4% paraformaldehyde, followed by dehydration through a series of increasingly concentrated ethanol solutions, 25%, 50%, 70%, and 100%.

Embryos were processed into paraffin, embedded, and sectioned. Prior to staining, slides with embryo sections were deparaffinized, baked for 30 min at 58°C, followed by rehydration through xylene and ethanol into phosphate buffered saline (PBS). For hematoxylin and eosin staining, samples were immersed in hematoxylin stain (VWR-#15204-152) for 8 minutes. Sections were placed under running tap water for 5 minutes, and then into acid alcohol (VWR-#15204-234) for 30 seconds. Slides were rinsed again under running tap water for 2 minutes, transferred to lithium carbonate for 45 seconds, and finally washed under tap water for 5 minutes. Sections were dipped in 80% ethanol 10 times, then stained in eosin for 40 seconds, followed by dehydration back through an ethanol series into xylenes. Finally, Permount Mounting Medium (VWR-#100496-550) was applied and specimens were covered with coverslips.

2.5 Immunostaining of Paraffin Sectioned and Whole Mount Embryos

Immunostaining of paraffin and whole mount tissues was carried out as previously described (Abashev, Metzler, Wright, & Sandell, 2017). For sections, antigen retrieval was performed and specimens were blocked in 5% lamb serum for 2 hours. Specimens were stained with primary antibodies overnight, washed, and stained with secondary antibodies for 1 hour. After washing off secondary antibodies, slides were stained 10 minutes with DAPI. Stained slides were mounted in Prolong Gold (Thermo Fisher P36930) and covered with coverslips. For whole mount immunostain, embryos were first permeabilized for 2 hours in in Dent's bleach (methanol:30% H₂O₂: DMSO, 4:1:1). After permeabilization, embryos were, re-hydrated through a graded series of methanol solutions into

PBS. Samples were blocked in whole mount blocking solution (0.1 M Tris pH7.5, 0.15 M NaCl with blocking reagent (Perkin Elmer FP1020)). Primary antibody hybridization was performed in blocking solution overnight 4°C with rocking. The next day, unbound primary antibody was removed with a series of 5 X 1 hour washes in PBS at room temperature. Specimens were then incubated overnight in fluorescently conjugated secondary antibody in whole mount blocking solution at 4°C with rocking. Unbound secondary antibody was removed by 3 x 20 minutes washes in PBS, followed by 4 hours nuclear stain with DAPI. Whole mount specimens were then post-fixed in 4% paraformaldehyde for 20 minutes. Stained embryos were then dehydrated through a graded series of methanol solutions into 100% methanol. Tissues were cleared by placing specimens in BABB (Benzyl alcohol: Benzyl benzoate, 1:2). Fluorescently immunostained embryos were then imaged by confocal microscopy on a Leica SP8 confocal microscope.

Primary antibodies used were Anti-SOX9 (Abcam, #185966) 1:200, Anti-myosin (DSHB, #BF-G6) 1:5, and Neuronal Class III β -Tubulin Monoclonal antibody (BioLegend-# 801201) 1:1000. Secondary antibodies were fluorescently conjugated: AlexaFluor 660 (Invitrogen), and AlexaFluor 546 (Invitrogen), each used at 1:300.

2.6 Assessment of Palate Fusion in *Ex Vivo* Cultured Maxillary Explants

Maxillary explant specimens from E13.5 embryos were micro-dissected free of mandible, tongue, and brain tissues. 1 to 3 explants were placed in a glass scintillation vial with 6 ml of BGJb culture medium (Thermo Fisher- # 12591038)

supplemented with 2.8 mg/ml glutamine, 6 mg/ml BSA and 1% Penicillin and streptomycin. The scintillation vial was flushed with a gas mixture of (50% O₂, 45% N₂, and 5% CO₂), and sealed using a silicone plug. The plugged vials were incubated on a Wheaton Mini Bench-top roller bottle system at a speed of 25 rpm, in a humidified 37°C incubator for 3 days. Each day, vials were re-flushed with the gas mixture for two minutes. At the end of the 3 day culture period, explants were fixed in 4% paraformaldehyde. Following fixation, specimens were whole mount stained with DAPI, and were imaged by fluorescent microscopy (Lisa L. Sandell et al., 2012).

2.7 MicroCT Analysis of Embryos

Whole E14.5 embryos were fixed in 4% paraformaldehyde overnight. Embryos were then equilibrated in 50% ethanol overnight, transferred to 70% ethanol for 2.5 hours, and then stained in phosphotungstic acid (PTA) stain for 8 days. The PTA stain solution is a heavy X-ray dense molecule that produces high contrast for soft tissues in X-ray analysis. After PTA staining, samples were then placed in 70% ethanol for 2 hours and then transferred to 100% ethanol for scanning. PTA stock solution was prepared as follows: 1 gram of dry PTA dry powder (VWR- #AA40116-22) was dissolved in 100 ml of distilled water to make 1% PTA stock solution. 30 ml of 1% PTA stock solution was dissolved in 70 ml of 100% ethanol to make a 0.3% PTA in 70% ethanol working stain solution.

For scanning, embryos were mounted inside a 1000 µl tapered pipette tip, sealed with paraffin wax at the bottom and filled with 100% ethanol. The embryo was gently wedged by gravity into the tapered end of the pipette, and 100% ethanol

was filled to the top of the pipette, which was then sealed with wax film. Another pipette tip was cut in half and wedged into sculptor's clay on the microCT platform to serve as a holder. The embryo in pipette tip was placed in the holder on the rotating platform of a Bruker micro-CT SkyScan 1174v2 compact X-ray micro-CT scanner. The settings used for scanning are as follows: Pixel size small, 6.84 μm , rotation of 0.3° with an average of 3 frames, 50 kV and 800 μA ; no filter was used. CT-an analysis software by Bruker was used for multi axis analysis of microCT scans dataset files. Additionally, Imaris software was used for surface rendering of isolated tongue volumes from the microCT data sets of control and mutant embryos.

2.8 X-gal Staining to Assess RARE-LacZ Reporter Gene Expression

To evaluate the tissue distribution of RA signaling, embryos carrying the RARE-lacZ reporter transgene were stained for β -galactosidase activity as whole mount specimens, imaged, and then processed and embedded through paraffin for sectioning. For whole mount staining, E10.5 RARE-LacZ reporter mouse embryos were harvested into ice cold PBS and fixed whole mount in 2% formalin plus 0.2% glutaraldehyde for 75 minutes on ice. After fixation, embryos were rinsed with β -galactosidase tissue rinse solution A (Millipore # BG-6-G), then washed in solution A for 30 minutes at room temperature. Embryos were then rinsed with β -galactosidase tissue rinse solution B (Millipore # BG-7-G) and then washed in solution B for 5 minutes at room temperature. Fixed embryos were then drained and placed in stain solution: β -galactosidase tissue stain base solution (Millipore #BG-8C) plus 1 mg/ml X-gal (Sigma-Aldrich #B4252-250MG).

Embryos were stained overnight at room temperature protected from light, then post-fixed in 4% paraformaldehyde overnight. Sections were counterstained with Nuclear Fast Red (VWR-#JTS635-1). After whole mount imaging, embryos were processed into paraffin and sectioned.

2.9 qPCR

Gene expression levels in cervical tissues were quantified by qPCR. Cervical tissues including the posterior pharyngeal arches (2nd-6th) were dissected out of E10.5 embryos via microdissection. Tissues were homogenized in RLT lysis buffer (Qiagen # 79216) with a syringe and needle. RNA was extracted from the isolated tissue using RNeasy Mini kit (Qiagen #74104) and converted to cDNA using SuperScript III First-Strand Synthesis System (Invitrogen #18080-051) using random hexamer primers. The gene specific qPCR primers listed below were used for amplification of RNA. All primer pairs used were validated to have efficiency between 90%-110%. *Gapdh* was used for normalization of gene expression. Data was evaluated by the $2^{-\Delta\Delta CT}$ method (Livak & Schmittgen, 2001). Significance was evaluated by two tailed Student's T-test assuming equal variance.

Table 2. Primers used for qPCR Gene Expression Analysis

<p><i>Gapdh</i> F: 5' ACAGTCCATGCCATCACTGCC 3', R: 5' GCCTGCTTCACCACCTTCTTG 3'</p>
<p><i>Hoxa1</i> F: 5' CCCAGACGGCTACTTACCAGA 3', R: 5' CATAAGGCGCACTGAAGTTCT 3'</p>
<p><i>Hoxb1</i> F: 5'GCCCCAACCTCTTTTCCCC3', R: 5' GACAGGATACCCCGAGTTTTG 3'</p>
<p><i>Tbx1</i> F: 5' CTGTGGGACGAGTTCAATCAG 3' R: 5' TTGTCATCTACGGGCACAAAG 3'</p>
<p><i>Hoxa2</i> F: 5' CTGAGTGCCTGACATCTTTTCC 3' R: 5' GTGTGAAAGCGTCGAGGTCTT 3'</p>
<p><i>Hoxa3</i> F: 5' GGAGGACAATTCGTCTCTTGG 3' R: 5' AGAACTTGTGGTTTGGACACTTC 3'</p>

2.10 Skeletal Stain with Alizarin Red and Alcian Blue

For skeletal staining of bone and cartilage, embryos were harvested at E16.5, and heads removed. Skin and organs were left intact. Embryos were rinsed in PBS and placed in ice cold 95% ethanol for one hour. Specimens were then transferred to fresh ethanol and rocked overnight at room temperature.

Specimens were then stained for cartilage and bone using Alcian Blue and Alizarin Red. The stain mixture was prepared in two separate stock solutions that were combined into a working mixture prior to staining. The stock solution of 0.4% Alcian blue in 70% ethanol was prepared as follows: 0.4 g of Alcian blue (VWR- #200063-912) was first added to 10 ml of 50% ethanol and placed in a 37°C water bath, with occasional swirling until dissolved. When Alcian blue was dissolved, 25 ml of water, and 65 ml of 95% ethanol were added. The stock solution of 0.5% Alizarin red S in water was prepared as follows: 0.5 g of Alizarin red S (VWR- #97062-616) was added to 100ml of water and swirled until dissolved. The combined working stain solution was then prepared from the two separate stock solutions. For 100ml of working stain solution, 5 ml of 0.4% Alcian blue in 70% ethanol was combined with 5 ml of glacial acetic acid (VWR- #BDH3098-3.8L), 70 ml of 95% ethanol, 20 ml of water, and 1 ml of 0.5% Alizarin red stock solution. Specimens were placed in the working stain solution for up to 8 days. At the completion of staining period, specimens were rinsed in water. The non-bone and cartilage tissues were cleared by incubating in a series of potassium hydroxide (VWR-#BDH9262-500G) and glycerol (VWR-#AAAA16205-AP) solutions for the following times: 4 hours in 2% KOH, then 30 minutes in

0.25% KOH, overnight in 20% glycerol/0.25% KOH, overnight in 33% glycerol/0.25% KOH and finally, overnight in 50% glycerol/0.25% KOH. Once specimens were cleared to reveal bone and cartilage, mandibles were carefully dissected away from the skull. Specimens were then imaged on a Leica stereomicroscope, and measured with Leica imaging software. Angle measurements were performed by analysis of images with Bruker Skyscan CT-an analysis program.

2.11 Ultrasound Imaging

Using a 2% concentration of isoflurane anesthesia, a pregnant mouse at E14.5 was placed in the supine position, a rectal temperature probe was placed, fur was removed and pre-warmed ultrasound gel was placed on the dam's abdomen. Once the dam's heart rate reached 500 bpm and the body temperature was 37°C, a 10-minute window was observed to allow equilibration to the isoflurane. Using the VisualSonics 770 ultrasound system, an RMV 707B probe was placed on the ultrasound gel covering the dam's abdomen. A sagittal-positioned embryo was located, and then monitored for a 20 minute period, during which the dam's body temperature was monitored and maintained. During this time, any movement of the embryo, namely, mouth opening or backward extension of the head and neck was documented. For each dam, only one embryo was monitored.

2.12 Statistical Analysis

Statistical analyses performed on the data were done using Excel software. Student's two-tailed T-test were used to compare two groups and significance

was determined by a P value of less than 0.05. Additionally, Chi Square test for Independence and Fisher's Exact Test for Independence in the case where an input value was zero, were used with P of less than or equal to 0.05 being significant. Results were presented as an average of values \pm standard error of the mean.

CHAPTER 3: RESULTS

3.1 Stage-Specific Inactivation of *Rdh10* Induces Secondary Cleft Palate

Vitamin A metabolism and RA production are essential for viability at early organogenesis stages of development, and deficiency of RA signaling from inception can result in embryonic lethality prior to palate morphogenesis (K Niederreither, Subbarayan, Dollé, & Chambon, 1999; L. L. Sandell et al., 2012; See, Kaiser, White, & Clagett-Dame, 2008; White et al., 1998). Therefore, in order to understand the requirement for Vitamin A metabolism and RA signaling during palate development, we performed stage-specific inactivation of *Rdh10* using a conditional allele (L. L. Sandell et al., 2012). Stage specific inactivation of *Rdh10* was achieved by Cre-mediated excision of a floxed allele of *Rdh10* via the tamoxifen-inducible Cre-ERT2 (Ventura et al., 2007).

Disruption of RA production at different embryonic stages can produce a variety of phenotypes (See et al., 2008; White et al., 1998). In a previous study, *Rdh10* was conditionally eliminated by Cre-ERT2 with tamoxifen administered at E7.5 to study the role of RA signaling in nasal airway development (Kurosaka, Wang, Sandell, Yamashiro, & Trainor, 2017). In the current study, we utilize the same mouse strains to conditionally inactivate RDH10 function by administration of

tamoxifen at E8.5. These experimental conditions, with tamoxifen administered at E8.5, have been previously validated to completely eliminate *Rdh10* RNA by E10.5, which attenuates RA signaling activity to 30% in comparison to the RA level in control embryos by E11.5 (Metzler et al., 2018).

To determine if RDH10 and endogenous RA are important for secondary palate formation, we assessed palate morphology in *Rdh10^{flox/+}* control and *Rdh10^{delta/flox}* mutant embryos at E16.5. Palates of embryos, with mandibles removed, were visualized by nuclear fluorescent staining (Fig. 6). Cleft of the secondary palate was observed in 36% of *Rdh10^{delta/flox}* mutant embryos (Fig. 6 B) (n=36). In contrast, cleft palate was not observed in any *Rdh10^{flox/+}* control embryos (Fig. 6 A) (n=37).

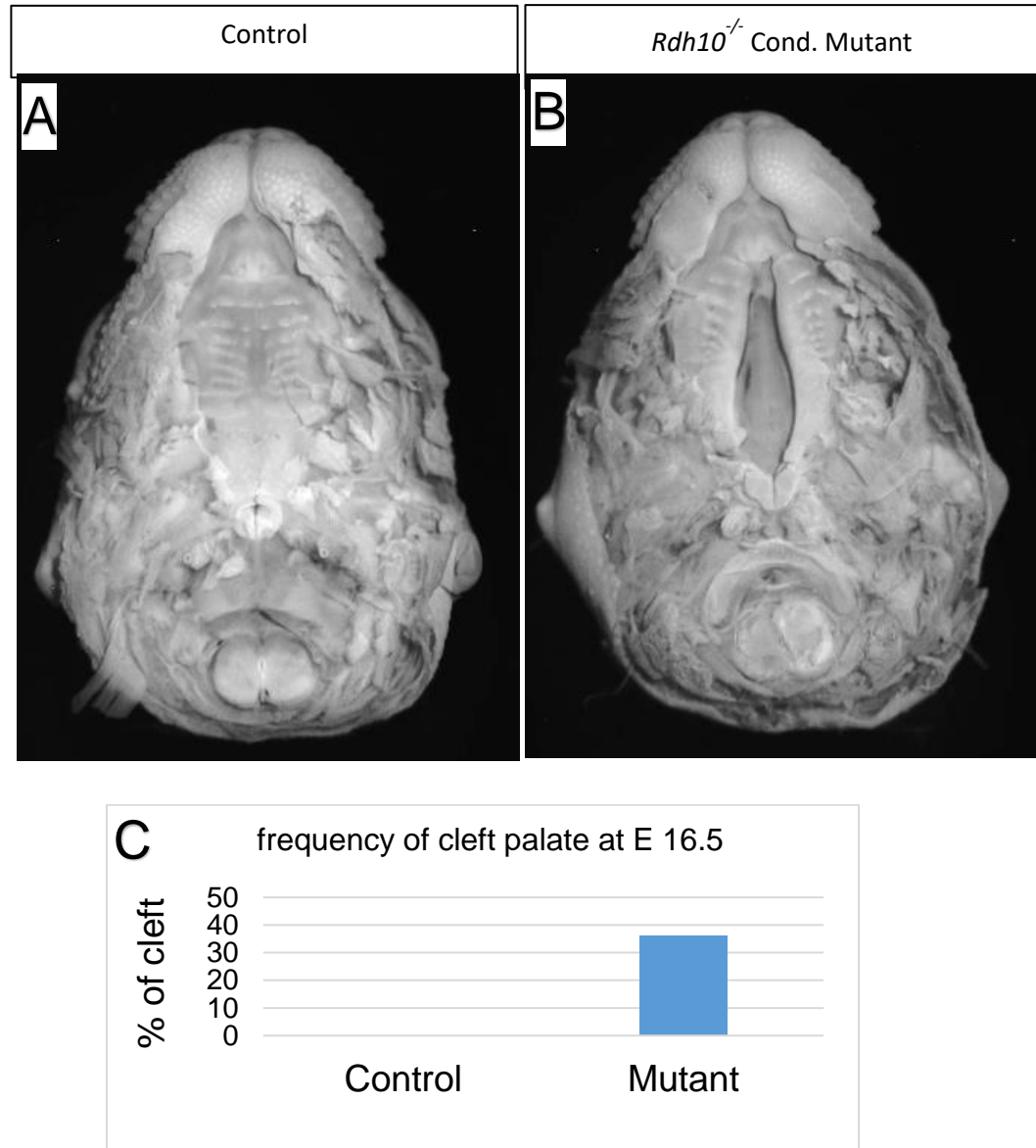


Figure 6. Morphological Comparison of Control Mutant Embryos. Nuclear fluorescent imaging of *Rdh10*^{fllox/+} control (A) and *Rdh10*^{delta/fllox} mutant (B) embryos at E16.5 reveals complete cleft of the secondary palate in mutant embryos. (C) The *Rdh10*^{delta/fllox} conditional inactivation model produces cleft palate at a frequency of 36% at E16.5 which is significant based off Fisher's Exact Test for Independence $p \leq 0.05$. Data generated in conjunction with Swetha Raja.

Overall cranial morphology of the *Rdh10^{delta/flox}* mutant embryos resembled that of *Rdh10^{flox/+}* control littermates (Fig. 7). Bone and cartilage staining of E16.5 embryos revealed that most of the cranial skeletal elements were present in mutant embryos. However, a notable difference was detected in the palatine bones of mutant embryos. In all control embryos the two opposing palatine bones had a feathery outgrowth that almost touched at the midline (Fig. 7 A, yellow arrowhead) (n=11/11). In contrast, in 50% of *Rdh10^{delta/flox}* mutant skulls, the feathery medial growth of the palatine bones was lacking and did not approach the midline (Fig. 7 B, yellow arrow) (n=4/8).

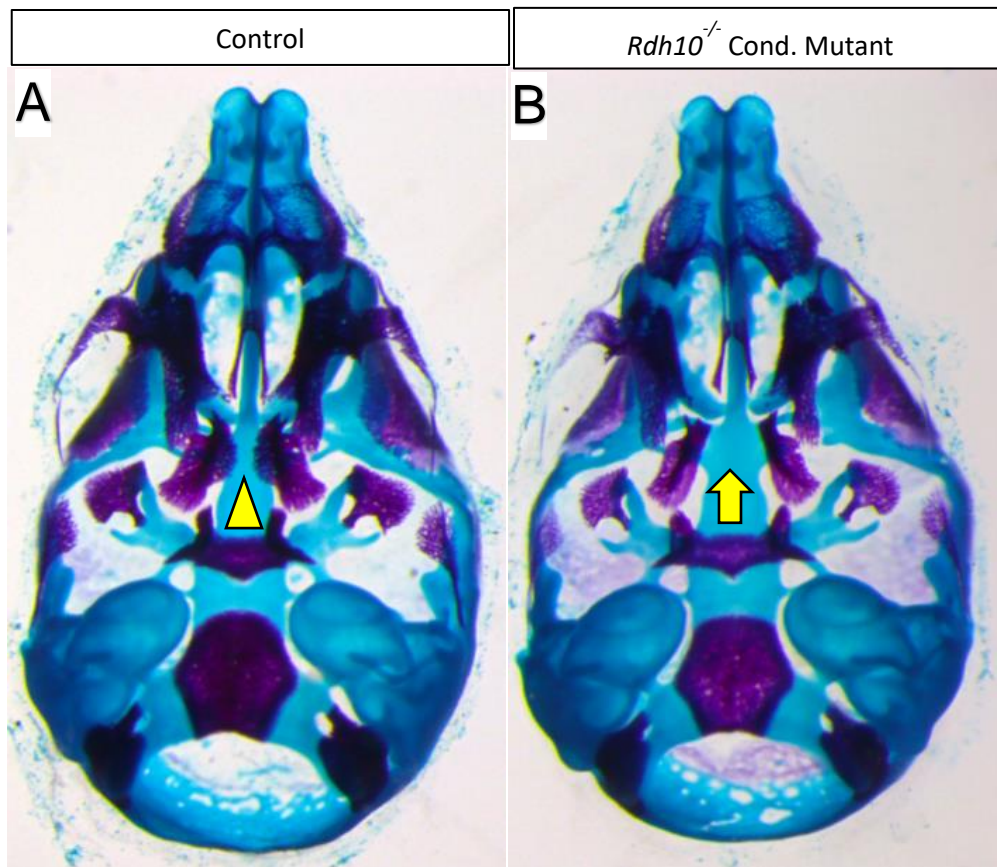


Figure 7. Bone and Cartilage Staining with Alizarin Red and Alcian Blue of E16.5 embryos. (A) Palatine bones of control embryos have grown towards the midline with feathery outgrowths (n=11/11). (B) In contrast, palatine bones of a subset of *Rdh10*^{delta/flox} mutant embryos remain lateral with no medial growth of bone towards the midline (n= 4/8).

To gain insight about the tissue architecture in cleft palates of *Rdh10^{delta/flox}* mutant embryos, we performed hematoxylin and eosin staining of paraffin sections (Fig. 8). At E13.5, the palate shelf morphology of *Rdh10^{delta/flox}* mutant embryos resembled that of *Rdh10^{flox/+}* control littermates, with palate shelves aligned vertically on either side of the tongue (Fig. 8 A, B). By E16.5, the palate shelves of *Rdh10^{flox/+}* control embryos have elevated and fused at the midline (Fig. 8 C, E, G). In contrast, the palate shelves of ~40% of *Rdh10^{delta/flox}* mutant embryos appear elevated but not grown towards the midline (Fig. 8 D, F, H). Together, these data reveal that *Rdh10^{delta/flox}* mutant embryos administered tamoxifen at E8.5 have reproducible cleft palate, demonstrating that this conditional inactivation model can be used to study the role of endogenous vitamin A and RA signaling in palate development.

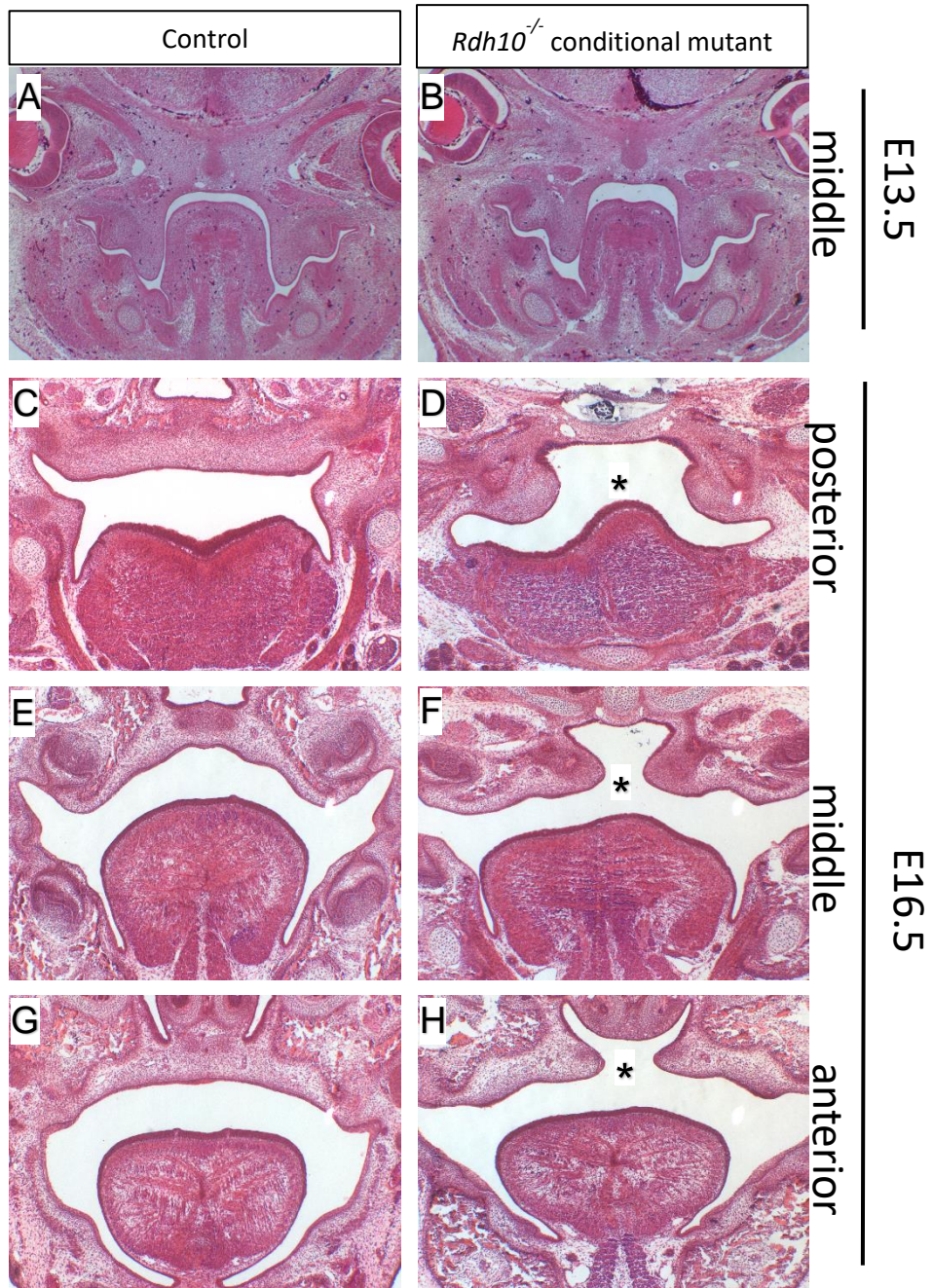


Figure 8. Histological Analysis of Control and *Rdh10*^{delta/flox} Mutant Embryos. Mid-palate coronal sections stained with hematoxylin and eosin reveal that control (A) and mutant (B) specimens are similar at E13.5, with palate shelves vertically oriented on either side of the tongue. (C-H) Hematoxylin and eosin stained sections of E16.5 embryos reveals the cleft palate defect in mutant embryos. At this stage palate shelves of control embryos have elevated, grown

towards the midline and fused in the posterior (C), middle (E), and anterior (G) palate. In contrast, palate shelves of mutant embryos are open and unfused in the posterior (D), middle (F), and anterior (H) palate. Black asterisks denote lack of medial contact of mutant palate shelves. Data generated in conjunction with Swetha Raja.

3.2 Culture of Isolated Maxillae *Ex Vivo* Suggests Extrinsic Defect Underlies Retinoid Deficient Cleft Palate

Cleft palate can be caused by defects intrinsic to the palate shelves, or by defects in other tissues that indirectly prevent palate closure. To determine whether cleft palate in retinoid deficiency occurs by a mechanism intrinsic or extrinsic to the palate shelves, we assessed fusion of maxillary explants cultured independently of the tongue and mandible. Maxillary tissues were isolated from E13.5 embryos, prior to shelf elevation (Fig. 9 A), and were placed in a rolling suspension culture for 72 hours to allow fusion to take place (Lan, Zhang, Liu, Xu, & Jiang, 2016). Under these conditions, palate shelf elevation and medial contact occurred in 79% of the maxillary explants from *Rdh10^{flox/+}* control embryos (Fig. 9 B, D) (n=19). Similarly, the maxillary explants from *Rdh10^{delta/flox}* mutant embryos also elevated and made medial contact at a rate of 77% (Fig. 9 C, D) (n=22). The two experimental groups are not statistically different, (Chi squared, $p > 0.05$).

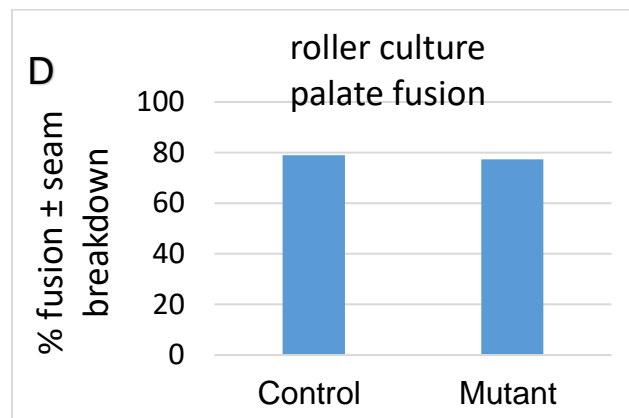
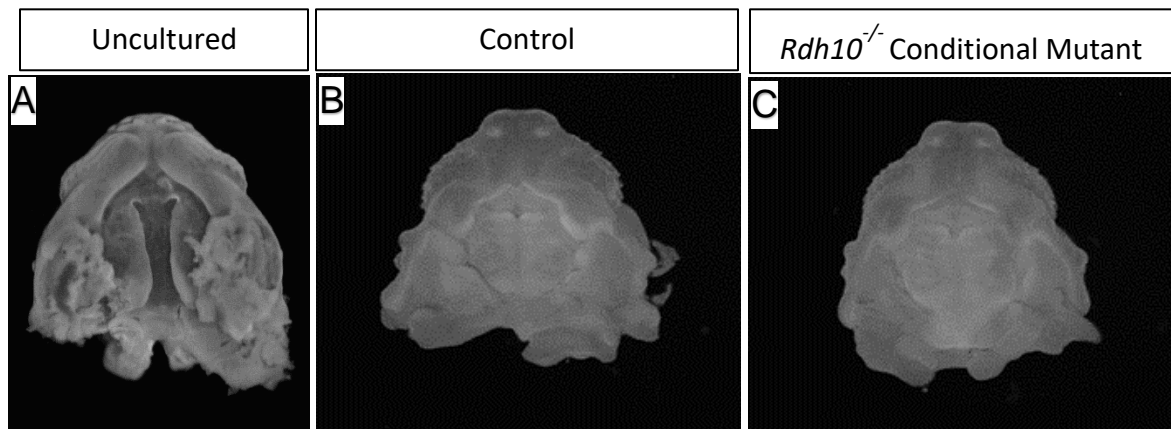


Figure 9. Three Day *Ex Vivo* Culture of Control and Mutant Maxillary Explants. (A) E13.5 maxillary explants with unfused palate shelves were dissected free of brain, mandible and tongue prior to *ex vivo* suspension culture. (B-C) Nuclear fluorescent imaging of cultured maxillary explants of *Rdh10*^{flox/+} control (B) and *Rdh10*^{delta/flox} mutant (C) embryos reveals apparent fusion of palate shelves following 72-hour culture period. (D) Graphical representation of frequency of apparent fusion for control and mutant explants. Chi square test for independence indicates the frequency of apparent fusion was not different between control and mutant explants, $p \geq 0.05$. Data generated in conjunction with Swetha Raja.

To determine if fusion occurred in cultured maxillae, subsets of cultured maxillary explants were examined histologically. Complete fusion with breakdown of the midline epithelial seam was observed in both *Rdh10^{flox/+}* control palate explants (Fig. 10 C) (n=2/6) and *Rdh10^{delta/flox}* mutant palate explants (Fig. 10 D) (n=5/6). Appearance of the midline epithelial seam, indicating a lack of complete fusion was apparent in *Rdh10^{flox/+}* control palate explants (Fig. 10 A) (n=4/6) and *Rdh10^{delta/flox}* mutant palate explants (Fig. 10 B) (n=1/6).

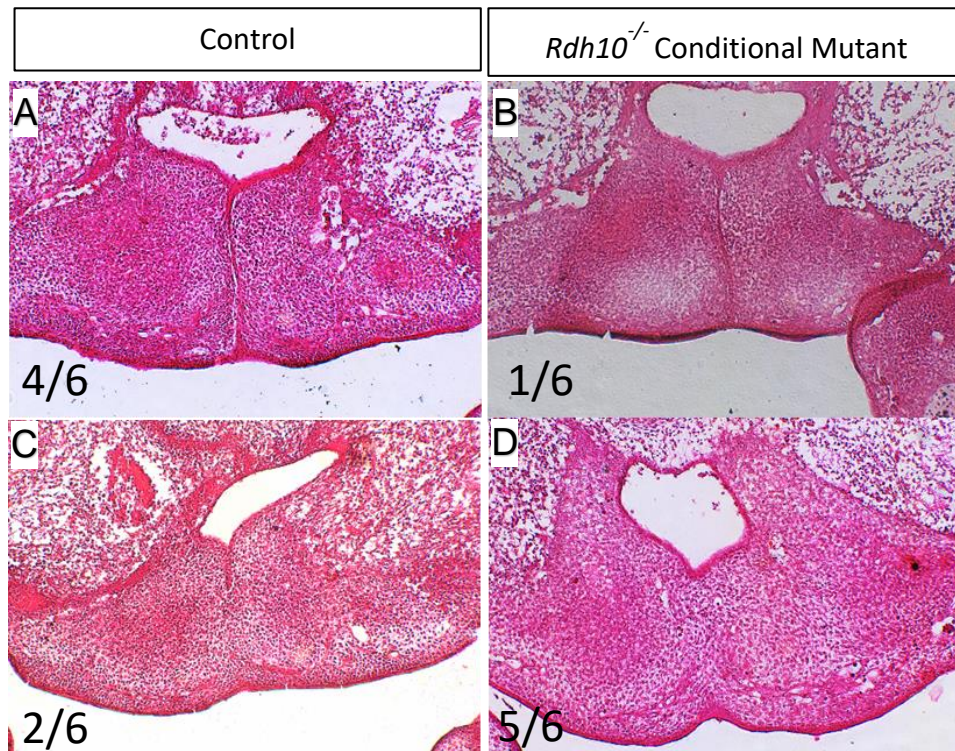


Figure 10. Histological Analysis of Control and *Rdh10*^{delta/flox} Mutant Embryos after Three-Day Culture. Hematoxylin and eosin staining of coronal sections through the cultured maxillae reveals complete fusion with breakdown of midline epithelial seam in some specimens. For sectioned control specimens 4/6 retained the midline epithelial seam (A), while 2/6 had evidence of fusion and loss of epithelial seam (C). For sectioned mutant specimens 1/6 retained the midline epithelial seam (B), while 5/6 had evidence of fusion and loss of epithelial seam (D). Data generated in conjunction with Swetha Raja.

These experiments do not unequivocally rule out a maxillary tissue defect as some biological processes might be altered by removing the mandible and tongue. However, an explant culture with the mandible and tongue removed is the best experiment available in the field to demonstrate that cleft palate is not caused by a defect intrinsic to the maxilla. The most likely explanation of these experiments is that these data indicate that the underlying mechanism of cleft palate in *Rdh10^{delta/flox}* mutant embryos is extrinsic to the palate shelves.

3.3 Retinoid Deficient Embryos do not Exhibit Micrognathia

One known extrinsic defect that can cause cleft palate is micrognathia, in which the small mandible crowds the tongue in the back of the oral cavity, preventing palate closure. In order to evaluate if retinoid deficiency causes micrognathia, we analyzed mandible size. After staining head specimens for bone and cartilage with Alizarin red and Alcian blue, mandibles were isolated by microdissection, imaged, and mandible length, width, and angle were measured (Fig. 11 A). Representative images of *Rdh10^{flox/+}* control (Fig. 11 B) and *Rdh10^{delta/flox}* mutant embryos at E16.5 (Fig 11 C) are shown.

No difference in mandible length was observed in *Rdh10^{delta/flox}* mutant embryos relative *Rdh10^{flox/+}* control littermates (Fig. 12 A). The mandibles of *Rdh10^{delta/flox}* mutant embryos had a very small but significant increase in width of the mandible relative to *Rdh10^{flox/+}* control littermates (Fig. 12 B). The increased width was reflected in a slight increase in angle of the mutant mandibles relative to controls (Fig. 12. C). No obvious differences were noted in bone or cartilage morphology

between the two groups. The similar size of mandibles of *Rdh10^{delta/flox}* mutant embryos and *Rdh10^{flox/+}* controls demonstrates that the retinoid deficient embryos do not have micrognathia. Thus, reduced mandible size is not the cause of secondary cleft palate in retinoid deficiency.

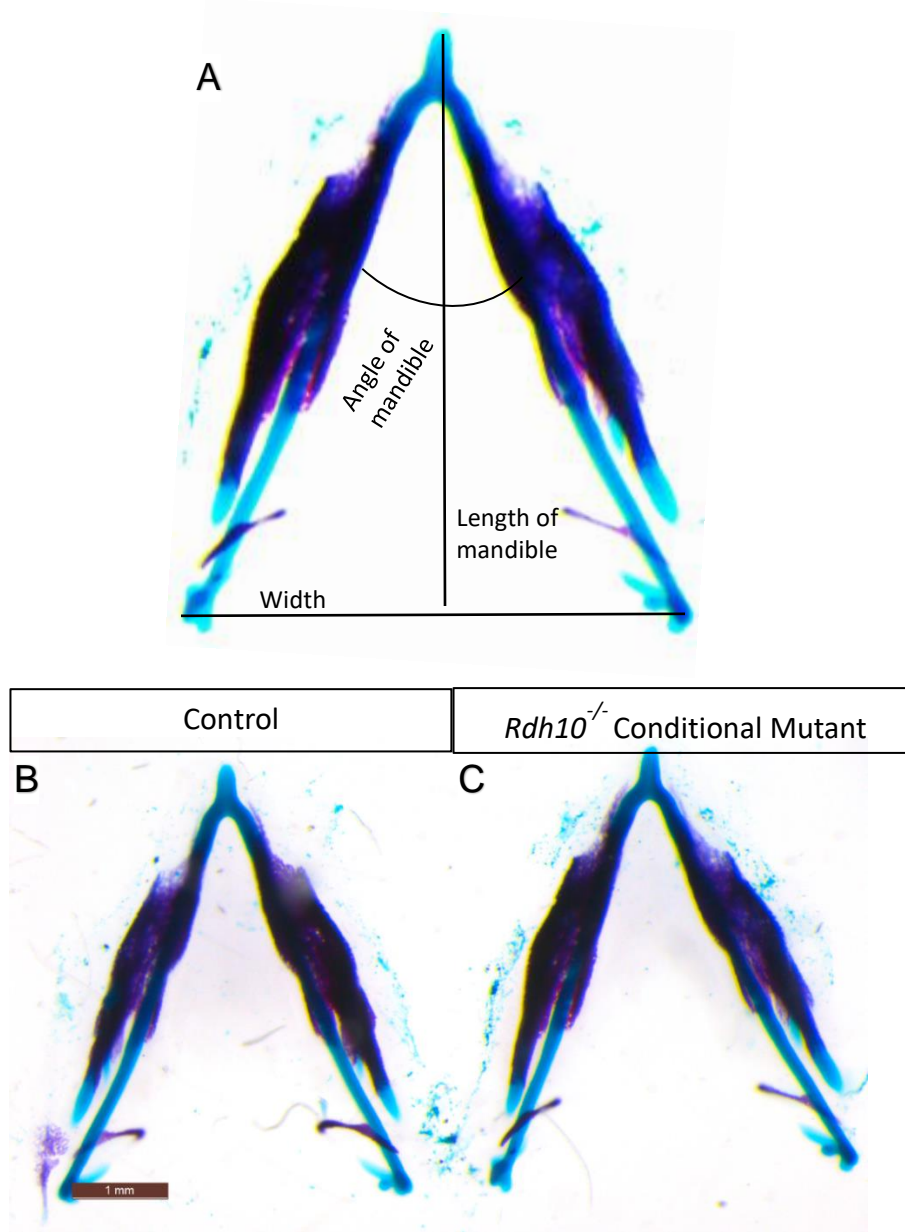


Figure 11. Alizarin Red and Alcian Blue Stain for Mandibular Analysis. (A) Mandibles were isolated from E16.5 embryos and stained with Alcian blue and Alizarin red to reveal bone and cartilage. Stained mandibles were imaged and measured for length, width, and angle. Mandible from an *Rdh10^{flox/+}* control (B) and *Rdh10^{delta/flox}* mutant embryos (C).

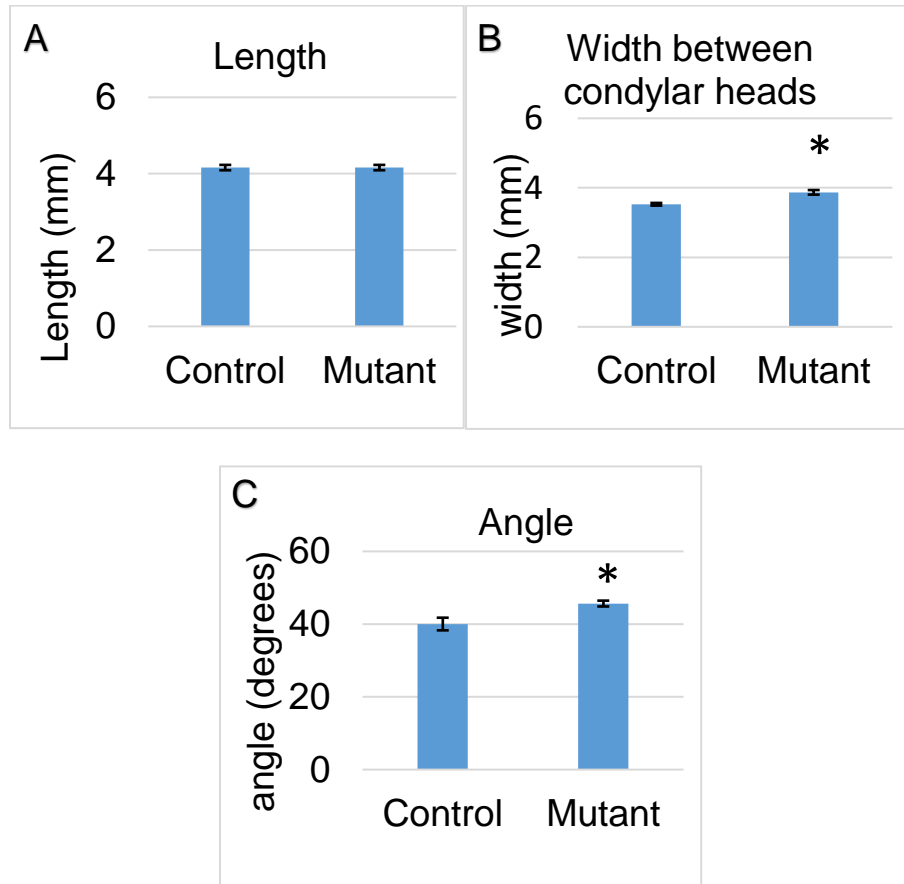


Figure 12. Measurements for Mandibular Size Analysis. The length of mandibles from mutant embryos was not significantly different from that of control embryos (A). Mutant mandibles were slightly wider than controls (B), with a larger interior angle measurement (C), $p \leq 0.05$, based on Student t-test.

3.4 The Tongue of *Rdh10*^{delta/flox} Mutant Embryos Obstructs Shelf Elevation

In order to gain insight about the causative morphological defects preceding cleft palate in retinoid deficient embryos, we performed microCT analysis on *Rdh10*^{flox/+} control and *Rdh10*^{delta/flox} mutant embryos at E14.5 (Fig. 13).

Reconstructed 3D matrix files were rendered to reveal sagittal, coronal, and transverse section images. Comparison of sagittal sections of *Rdh10*^{flox/+} control (Fig. 13 A) and *Rdh10*^{delta/flox} mutant (Fig. 13 B) embryos revealed a difference in tongue position. Tongues of control embryos were relatively flat (single blue arrow, n=4/4), while tongues of mutant embryos were arched in the posterior (double blue arrows, n= 5/5). In control embryos palate shelves were visible along their length, indicating that the shelves had grown toward the midline, whereas in mutant embryos, posterior palate shelves were not visible near the midline. Comparison of coronal sections revealed that the palate shelves of *Rdh10*^{flox/+} control embryos (Fig. 13 C, C') were elevated horizontally above the flattened tongues (n=3/4 both shelves elevated, n=1/4 one shelf elevated), whereas *Rdh10*^{delta/flox} mutant embryos (Fig. 13 D, D') had vertical palate shelves trapped on either side of the arched tongue (n=4/5 both shelves vertical and trapped). Transverse sections at the level of the tongue of the control embryo (Fig. 13 E) reveals that the tongue was elongated and lying completely under the palate shelves, which were out of view. In contrast, in *Rdh10*^{delta/flox} mutant embryo's (Fig. 13 F) palate shelves were visibly trapped at the posterior aspect of the tongue. Together these data reveal that *Rdh10*^{delta/flox} mutant embryos have mal-positioned tongues that obstruct palate elevation at E14.5.

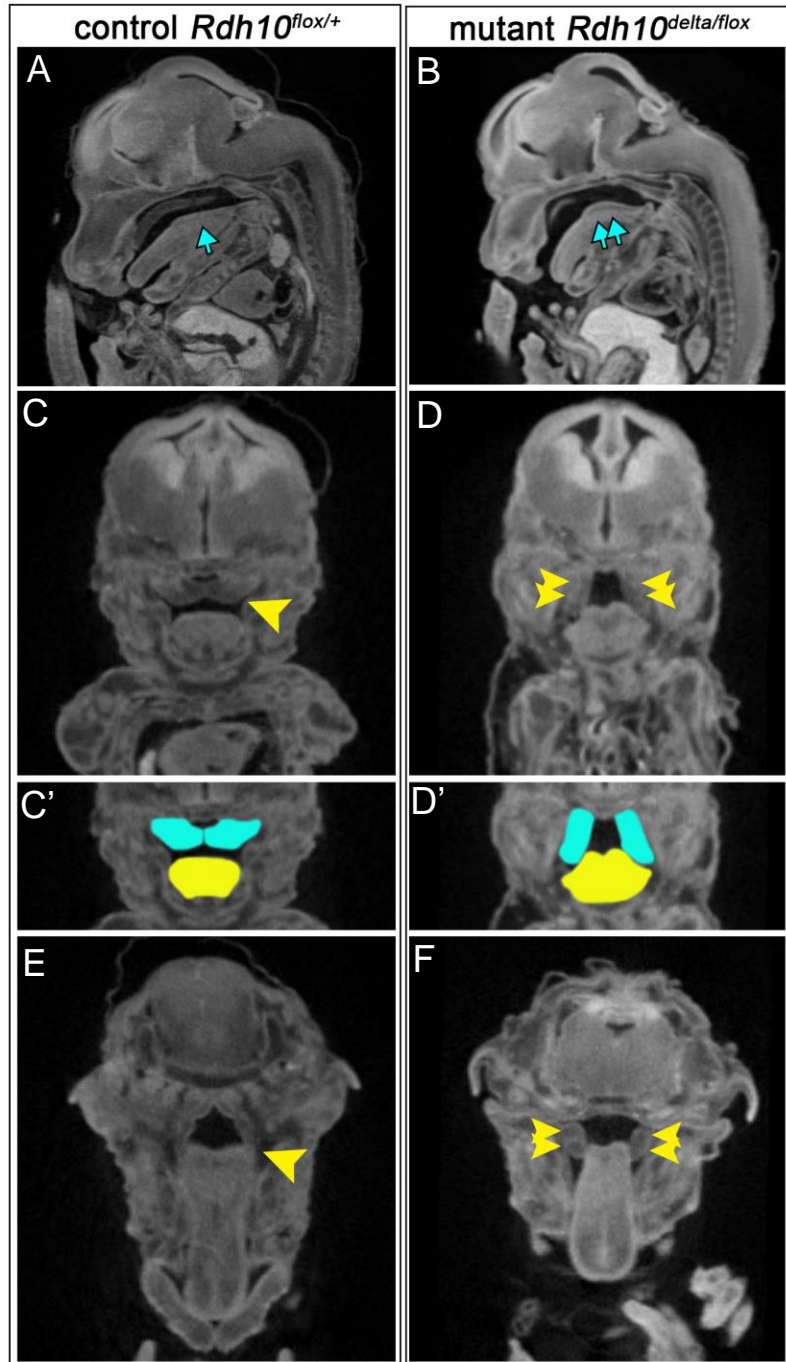


Figure 13. Analysis of Embryo Morphology by microCT. Scans reveals *Rdh10^{delta/flox}* mutants have abnormally positioned tongues that obstruct palate shelf elevation. MicroCT scans of E14.5 *Rdh10^{flox/+}* control (A, C, C' and E) and *Rdh10^{delta/flox}* mutant (B, D, D' and F) embryos. Sagittal view at the midline shows the tongue of control embryo lies flat under the posterior palate shelf (A, single

blue arrow, n=5/5), while the mutant embryo tongue is arched in the back of the oral cavity (B, double blue arrow, n=6/6), with no overlying palate shelf visible. (C) Coronal view of control embryo shows that palate shelves have elevated over the tongue and contact at the midline (single yellow arrowhead, n=4/5 both shelves elevated, n=1/5 one shelf elevated). (D) In contrast, coronal view of mutant embryo reveals the palate shelves oriented vertically, appearing obstructed by the arched tongue (double yellow arrowhead, n=5/6). (C') Color coded image of (C) with blue palate shelves elevated over a yellow flattened tongue. (D') Color coded image of (D) with blue palate shelves trapped vertically on each side of the tongue. (E) Transverse section at the level just above the tongue reveals control tongue has flattened out underneath the palate shelves that are elevated out of view (single yellow arrowhead). (F) Transverse section above mutant tongue reveals the posterior palate shelves wedged laterally on either side of the tongue (double yellow arrowhead).

To determine if the tongue obstruction in that *Rdh10^{delta/flox}* mutant embryos resulted from increased tongue volume, we measured tongue volume in control and mutant embryos by volume rendering microCT datasets (Fig. 14). Volumetric analysis showed that *Rdh10^{delta/flox}* mutant tongues ((Fig. 14 B, D, F) were smaller than the tongues of control (Fig. 14 A, C, E) littermates (Fig. 14 G). These data indicate that tongue obstruction of the palate shelves is not caused by increase tongue volume.

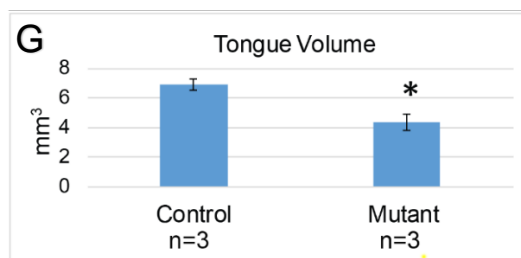
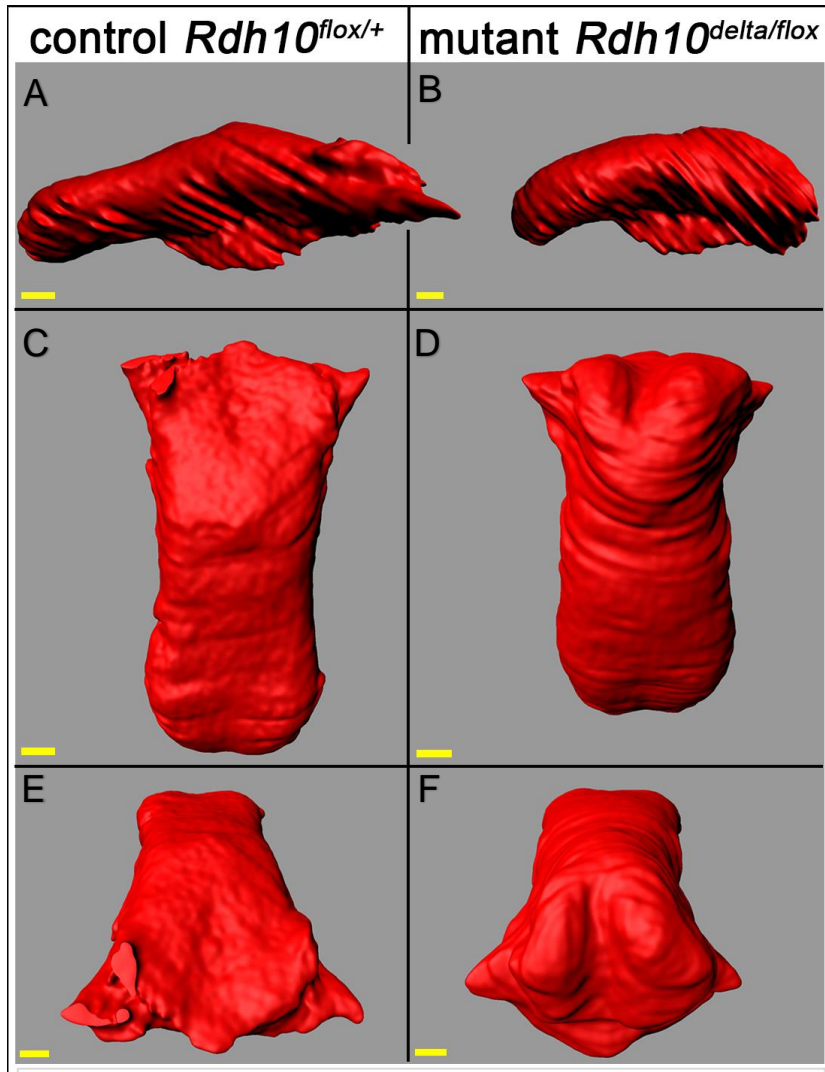


Figure 14. Volumetric Analysis of Control and Mutant Tongues. Volume rendering of the control (A, C, E) and mutant (B, D, F) tongues gives a sagittal (A, B), dorsal (C, D) and posterior view (E, F) of the tongue morphology. (G) The volumetric analysis shows the mutant tongues are smaller in volume, $p \leq 0.05$. Yellow scale bars in tongue volumetric analysis (G-L) are 200 μm in length.

Our observation of abnormal arched and contracted appearance of tongues in *Rdh10^{delta/flox}* mutant embryos led us to evaluate the intrinsic tongue muscles (Fig. 15). We performed immunostaining for the muscle marker myosin on coronal sections of E14.5 *Rdh10^{delta/flox}* mutant (Fig. 15 B) and *Rdh10^{flox/+}* control (Fig. 15 A) embryos. No defect was observed in the intrinsic tongue muscles in mutant embryos relative to control littermates. All intrinsic muscles of the tongue, as well as the genioglossus fibers, appeared to be present and normal in the *Rdh10^{delta/flox}* mutant embryos.

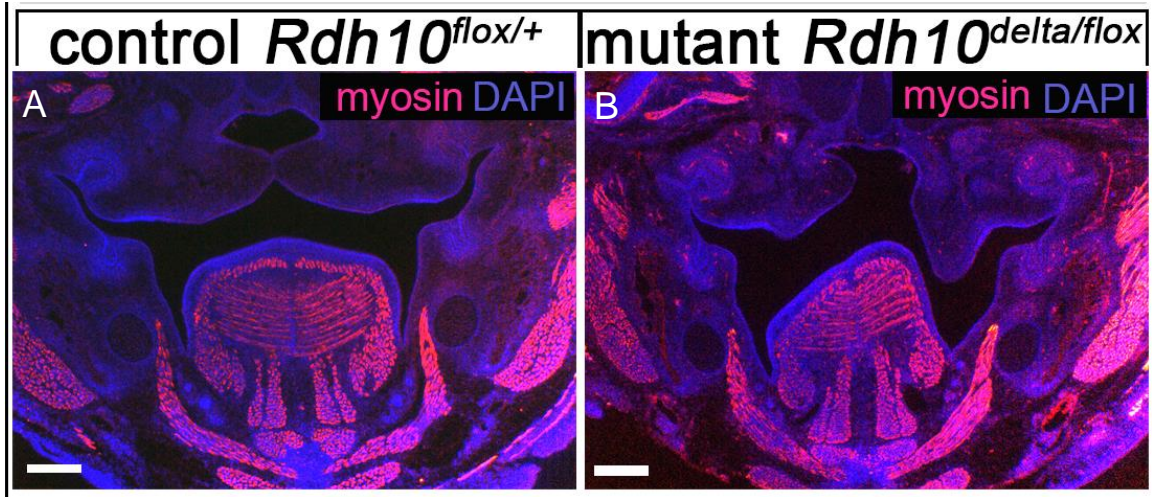


Figure 15. Muscle Morphology Analysis of Control and Mutant Embryos. Immunofluorescent staining for myosin on E14.5 coronal sections of control (A) and mutant (B) tongues, reveals mutant tongue musculature is grossly normal. White scale bars are 1 mm in length.

Collectively, these results indicate the morphogenesis of tongue musculature is grossly normal in retinoid deficient embryos, suggesting the abnormal tongue shape does not result from aberrant muscle morphogenesis.

3.5 *Rdh10*^{delta/flox} Mutant Embryos have Defects in Motor Nerves of the Posterior Pharyngeal Arches

Having observed that *Rdh10*^{delta/flox} mutant embryos had mal-positioned tongues obstructing palate shelf elevation, we next investigated the possibility that the mutant arched tongue phenotype was associated with defects in tongue motor nerves. To assess motor nerve development in control and mutant embryos we performed whole mount immunostaining for TUBB3 neurons of E11.5 embryos (Fig 16, Fig. 17).

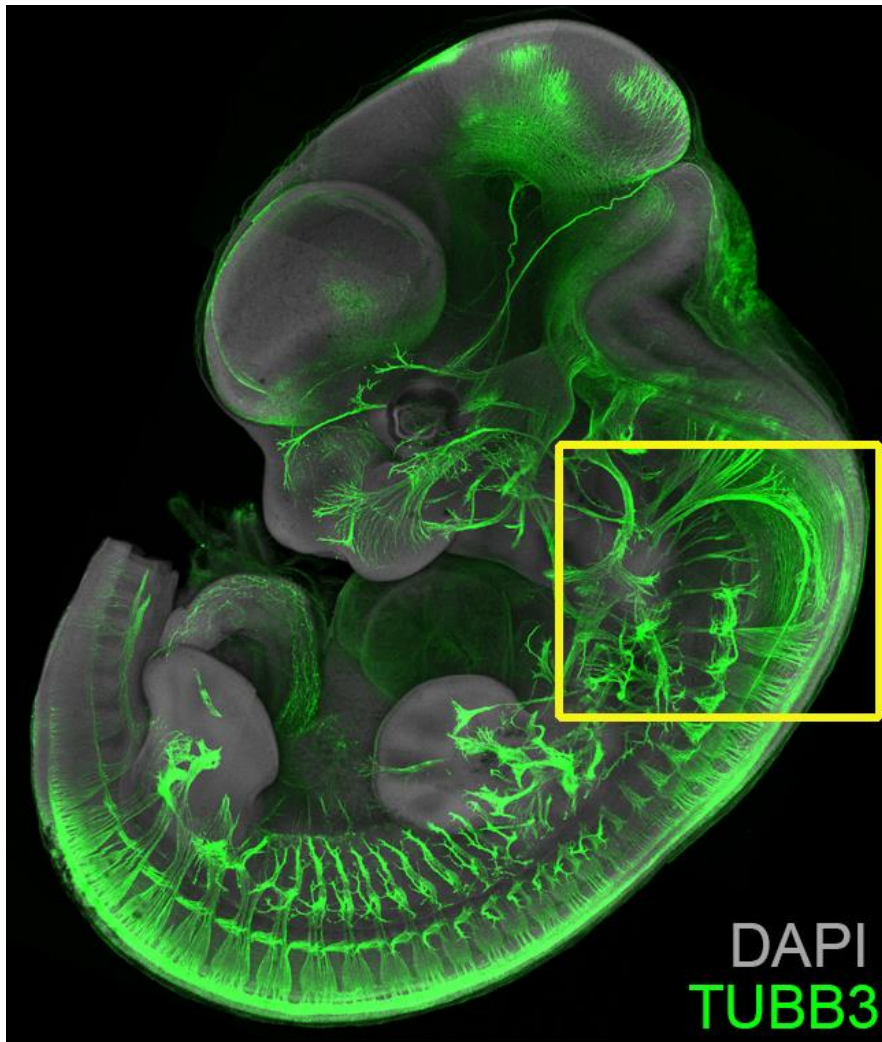


Figure 16. Schematic of Nerve Staining of an E10.5 Embryo. Wild type E11.5 embryo immunostained whole mount for TUBB3 reveals all nerves. Yellow box defines pharyngeal region shown in following figures.

The muscles of the tongue are innervated by the hypoglossal nerve (CN XII), which supplies their motor function. CN XII outgrows from the ventral neural tube anterior to cervical spinal nerve 1 (C1). C1 travels posteriorly to plex with the ventral rami of the cervical spinal nerves (C1-C4) before climbing to give motor supply to structures of the pharyngeal region involved in swallowing. In *Rdh10^{flox/+}* control embryos (Fig. 17 A, C) CN XII fibers were clearly visible as an independent tract outgrowing toward the tongue, with C1 traveling posteriorly and disappearing behind the anterior dorsal root ganglion to join the cervical plexus. In contrast, *Rdh10^{delta/flox}* mutant embryos (Fig. 17 B, D) exhibited a dysmorphic outgrowth of CN XII, which fused abnormally with C1. In such cases C1 did not travel posteriorly to join the cervical plexus, but rather, fused directly with CN XII. This abnormal fusion of C1 and CN XII was observed in 50% of the mutant nerves (n=4/8), while it was never found in the control littermate nerves (n=0/14) (Fig. 17 E).

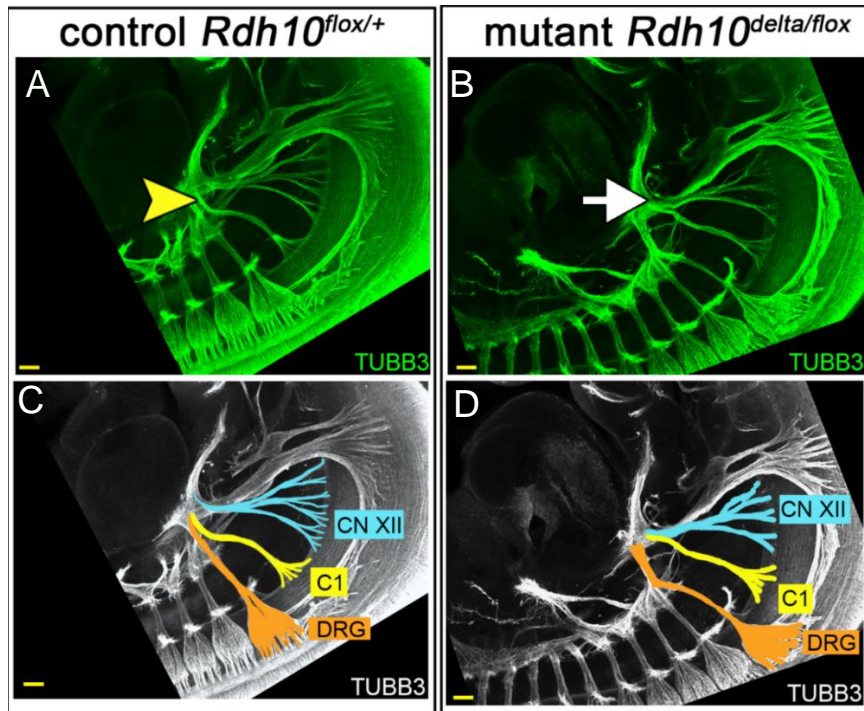


Figure 17. Nerve Outgrowth Analysis of CN XII and C1. (A) In *Rdh10^{flox/+}* control embryos (A, C) motor nerve C1 routes posteriorly to plex with other cervical nerves behind the anterior-most dorsal root ganglion before climbing superiorly (yellow arrowhead). (B) In *Rdh10^{delta/flox}* mutant embryos (B, D) the motor nerve C1 does not track posteriorly behind the anterior-most dorsal root ganglion, but is mis-routed to fuse directly with CN XII (white arrow). (C, D) Color coded images of control (C) and mutant (D) embryos to highlight the mis-routing of C1 fusing with CN XII in mutant embryos. (E) The frequency of aberrant fusion of C1 to CN XII was 50% of mutant nerves (n=4/8). Aberrant fusion was never observed in nerves of control embryos (n=0/14). All scale bars are 100 μ m in length.

The dysmorphic fusion of C1 to CN XII likely affects function of the muscles innervated by these nerves. Direct targets of CN XII include the muscles of the tongue, and direct targets of C1 include the geniohyoid and thyrohyoid muscles, which work synergistically to move the hyoid bone and larynx during swallowing. These data suggest that abnormal motor nerve patterning could impact movement of the tongue and pharyngeal swallowing apparatus.

3.6 Retinoid Deficient Embryos Develop Defects in the Pharyngeal Skeleton

The observation that mal-positioning of the tongue obstructs palate shelf elevation in *Rdh10^{delta/flox}* mutants, prompted us to investigate the pharyngeal skeleton; the hyoid bone, and the thyroid and cricoid cartilages, which function to anchor the muscles of the tongue, mandible, and pharynx. We examined the pharyngeal skeleton in E16.5 *Rdh10^{delta/flox}* mutant (Fig. 18 B) and *Rdh10^{flox/+}* control (Fig. 18 A) embryos by Alcian blue staining. *Rdh10^{delta/flox}* mutant embryos had morphological defects in all pharyngeal skeletal elements, including ectopic fusion of the hyoid primordium to the laryngeal prominence of the thyroid cartilage, and an abnormal gentle “M” shaped hyoid primordium (Fig. 18 B, black arrow). The striking pharyngeal skeleton phenotypes observed *Rdh10^{delta/flox}* mutant embryos parallel those previously described for other models of retinoid deficiency (Luo, Sucov, Bader, Evans, & Giguere, 1996; See et al., 2008; Vermot, Niederreither, Garnier, Chambon, & Dolle, 2003).

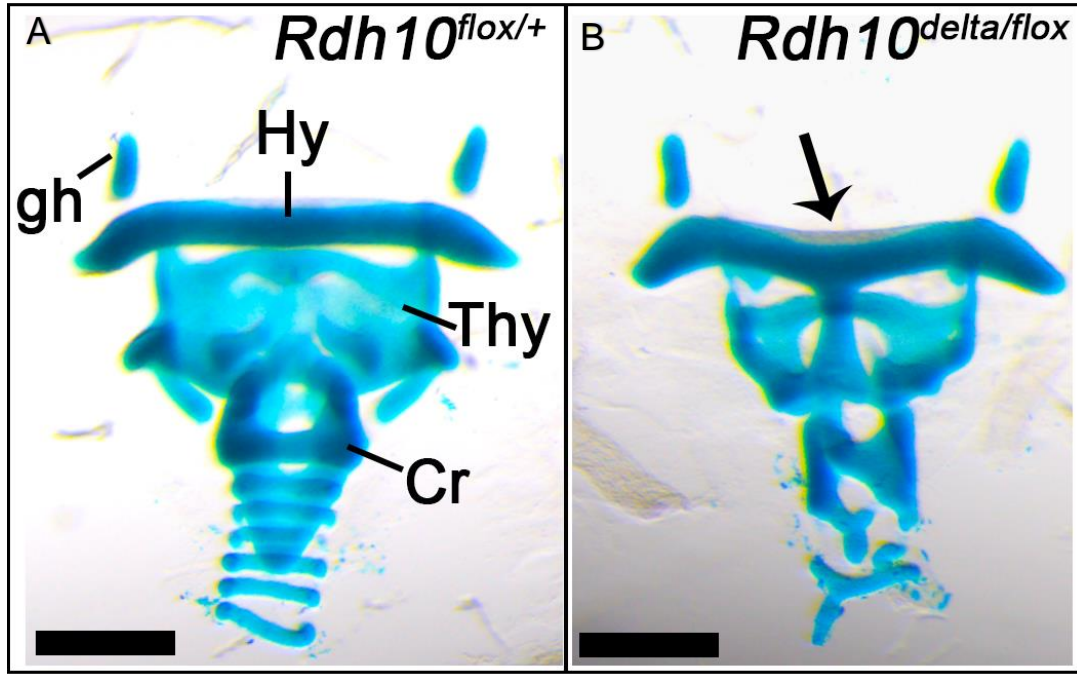


Figure 18. Pharyngeal Skeleton Analysis with Alcian Blue Staining. *Rdh10^{delta/flox}* mutant embryos have defects in pharyngeal skeletal primordia. Skeletal preparation of isolated pharyngeal cartilages from *Rdh10^{flox/+}* control embryos (A) and *Rdh10^{delta/flox}* mutant embryos (B) at E16.5. (B) In mutant embryos the laryngeal prominence of the thyroid cartilage was abnormally fused to the primordium of the hyoid bone (black arrow). (B) Abnormal fusion of the thyroid cartilage to hyoid primordium was observed in all mutant embryos (n=9/10), but was never detected in control samples (n=0/12), (Fischer's Exact test for independence, $p \leq 0.05$). (B) In addition to the abnormal fusion, the hyoid primordia in mutant embryos also had a distinctive "M" shape (black arrow, n=9/10), compared to the hyoid of control embryos, which were straighter between the horns (n=0/12), (Fischer's Exact test for independence, $p \leq 0.05$). Hy=hyoid bone primordium, Thy=thyroid cartilage primordium, Cr=cricoid cartilage primordium, gh= greater horn of the hyoid bone primordium.

Table 3. Frequencies of Pharyngeal Cartilage Defects

Hyoid to Thyroid fusion			
	separate	fused	Total
<i>Rdh10^{flox/+}</i>	12	0	12
<i>Rdh10^{delta/flox}</i>	1	9	10
Hyoid shape			
	Normal	Abnormal	Total
<i>Rdh10^{flox/+}</i>	12	0	12
<i>Rdh10^{delta/flox}</i>	1	9	10

We next examined the attachment of the tongue muscles to the pharyngeal cartilages in control and *Rdh10^{delta/flox}* mutant embryos via paraffin section and immunostaining (Fig. 19). E14.5 embryos were sectioned transversely at the level of the hyoid bone, and stained for myosin to visualize muscle primordia, and SOX9 to visualize cartilage primordia. In control embryos (Fig. 19 A), myosin positive fibers were directed toward, and abutted into, the greater horn of the hyoid, suggesting muscle attachment to the bone primordium (Yellow arrowheads). In contrast, in *Rdh10^{delta/flox}* mutant embryos (Fig. 19 B), myosin positive fibers did not appear to contact the greater horn of the hyoid primordium (Yellow astericks). The lack of definitive muscle contact to the malformed hyoid primordium suggests that the muscle anchoring attachment could be impaired in mutant embryos.

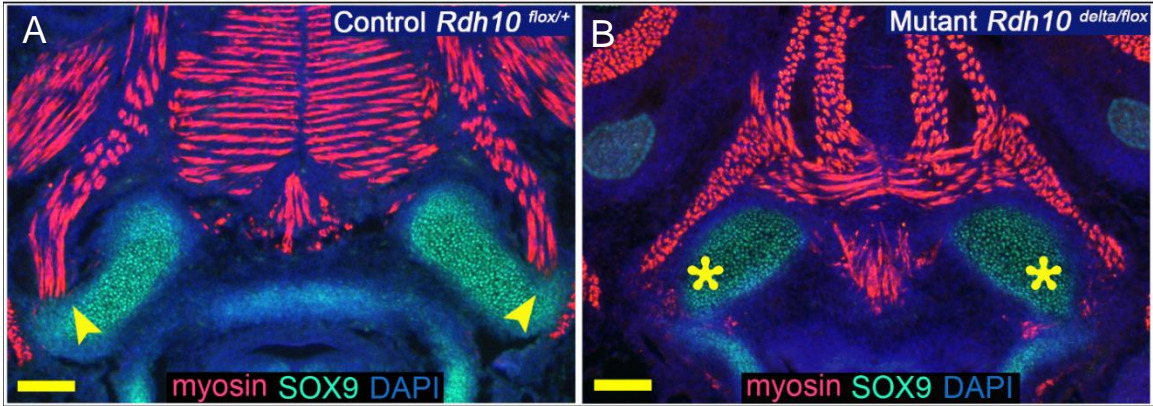


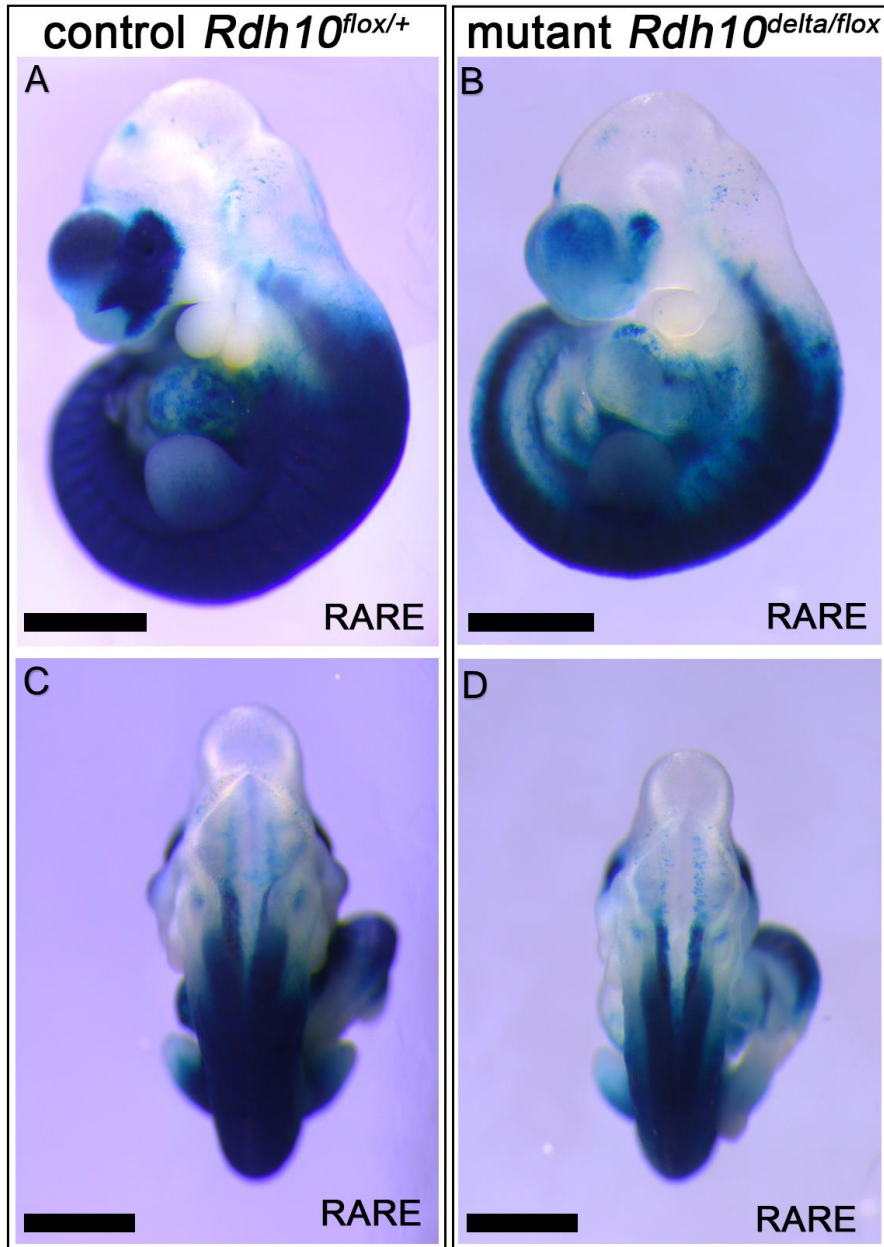
Figure 19. Muscle Attachment Analysis of Tongue Musculature to the Hyoid Bone. Transverse sections through tongues of E14.5 control (A) and mutant embryos (B) were immunostained with antibodies against myosin (muscle primordia) and SOX9 (cartilage primordia). (A) In control embryos, muscle contact to the greater horn of the hyoid was detected (yellow arrowheads). In contrast, in mutant embryos, muscle contact to the dysplastic greater horns of the hyoid was not evident (B, yellow asterisks). Black scale bars are 500 μm in length. Yellow scale bars are 100 μm in length.

The observation that *Rdh10^{delta/flox}* mutant embryos have dysplastic pharyngeal cartilages, with reduced or absent muscle contact, suggests that defects in patterning the pharyngeal skeleton could hinder movement of the tongue and mandible in these embryos.

3.7 Conditional Inactivation of *Rdh10* Disrupts Pharyngeal Anterior-Posterior Patterning Genes, Consistent with Other RA Deficiency Models.

Deficient RA signaling is known to disrupt expression of pharyngeal patterning genes. To validate that *Rdh10^{delta/flox}* embryos, have reduced RA signaling and altered patterning gene expression in pharyngeal tissues, we examined the spatial location of RA signaling, and expression of *Hoxa1*, *Hoxb1*, and *Tbx1*, in control and mutant embryos.

For the experimental *Rdh10^{delta/flox}* mutant system utilized here, in which tamoxifen is administered at E8.5, we have previously demonstrated that RA signaling is attenuated to 30% that of control embryos by E11.5 (Metzler et al., 2018). Here we use the RARE-LacZ reporter transgene to assess the spatial distribution of RA signaling activity at E10.5 (Fig. 20). Comparison of whole mount RARE-LacZ staining in *Rdh10^{flox/+}* control embryos (Fig. 20 A, C) with *Rdh10^{delta/flox}* mutants (Fig. 20 B, D) reveals that mutant embryos have reduced RA signaling, particularly in the ventral tissues (n=3 mutant embryos). Analysis of paraffin sections reveals a reduction of RA signaling in somitic mesoderm and posterior pharyngeal arch mesenchyme in mutant embryos (Fig. 20 F, H) relative to controls (Fig. 20 E, G).



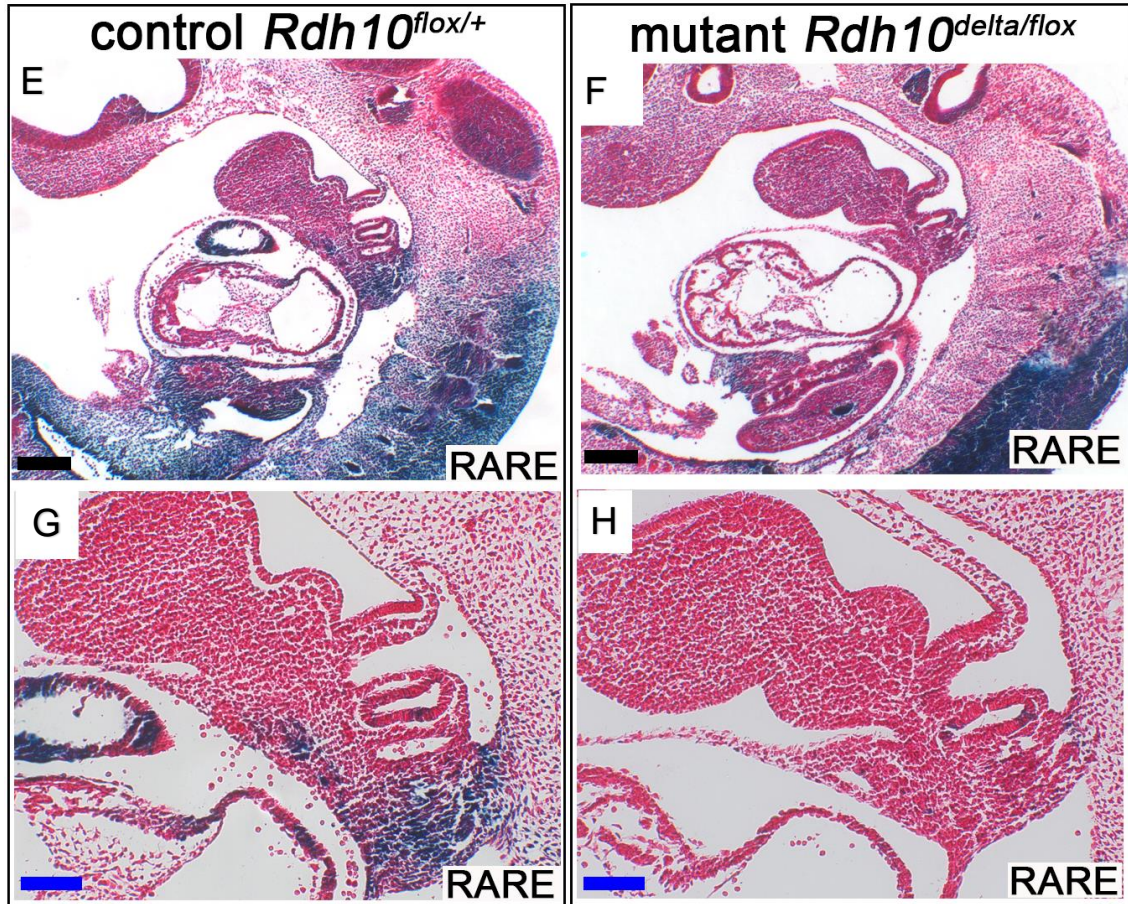


Figure 20. RARE LacZ Analysis with Whole Mount Specimens and Histology. Consistent with RA deficiency models *Rdh10^{delta/flox}* inactivation reduces RA signaling and modifies expression of *Hoxa1*, *Hoxb1* and *Tbx1* in pharyngeal tissues. E10.5 embryos carrying the RARE-LacZ reporter transgene were stained whole mount with x-gal to show the pattern of RA signaling. (A, C) *Rdh10^{flox/+}* control embryo in side (A) and dorsal view (C). (B, D) Diminished RA signaling in *Rdh10^{delta/flox}* mutants is evident in side view (B). (E-H) Whole mount stained embryos were sectioned to view the distribution of RA signaling in pharyngeal arch tissues. In the control embryo, RA signaling is active in the somitic mesoderm and pharyngeal mesenchyme (E, G). In contrast, in *Rdh10^{delta/flox}* mutant embryos, somitic mesoderm and pharyngeal mesenchyme are predominantly negative for RA signaling (F, H). Black scale bars are 1 mm in length. Blue scale bars are 100 μ m in length.

RA is known to regulate expression of pharyngeal patterning genes (Bel-Vialar, Itasaki, & Krumlauf, 2002; Deschamps & van Nes, 2005; Diez del Corral & Storey, 2004; Gavalas et al., 1998; White, Highland, Kaiser, & Clagett-Dame, 2000; White et al., 1998). To understand the etiology of the pharyngeal abnormalities in retinoid deficient embryos, we examined expression of key pharyngeal patterning genes in control and mutant embryos (Fig. 22). To that end we performed qPCR for *Hoxa1*, *Hoxb1*, and *Tbx1* on isolated cervical tissues that included the 2nd-6th arches of E10.5 embryos (Fig. 21).

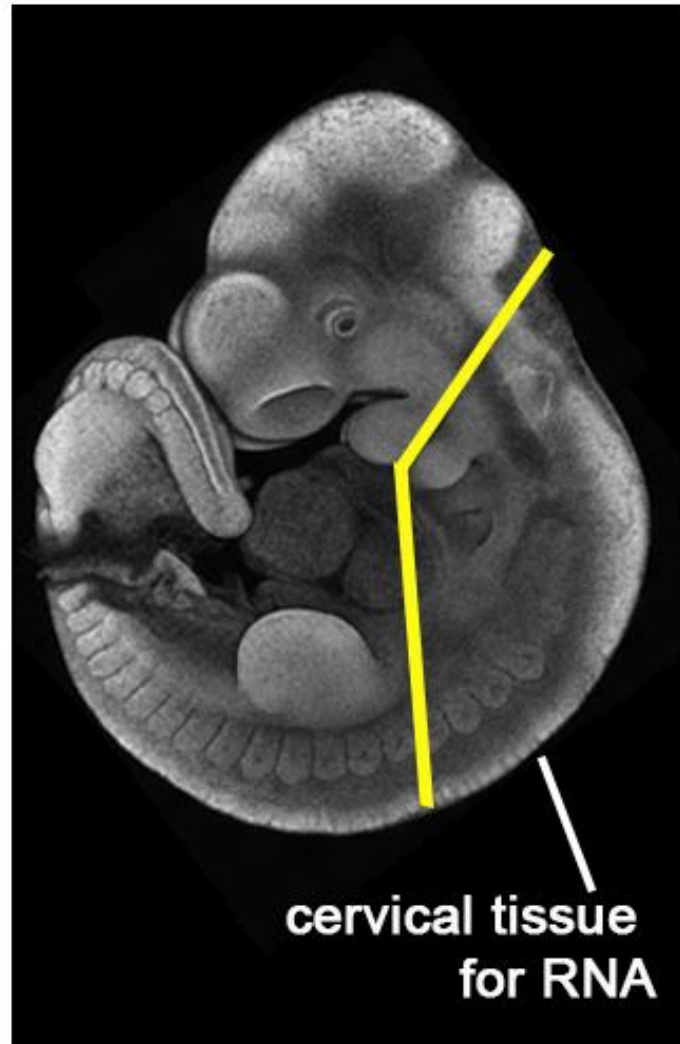


Figure 21. Schematic Representation of the Region that was used for qPCR Analysis.

Hoxa1 and *Hoxb1*, both of which are directly regulated by RA signaling, were significantly downregulated in *Rdh10^{delta/flox}* mutant embryos to 60% that of controls (Fig. 22 A, B). Conversely, *Tbx1*, a transcription factor known to be negatively regulated by RA signaling, was increased in *Rdh10^{delta/flox}* mutant pharyngeal tissues to 130% the level of controls (Fig. 22 C). We also examined expression of *Hoxa3*, a gene required for development pharyngeal cartilages (Chojnowski, Trau, Masuda, & Manley, 2016; Mulder, Manley, & Maggio-Price, 1998), however, no significant difference was observed (data not shown).

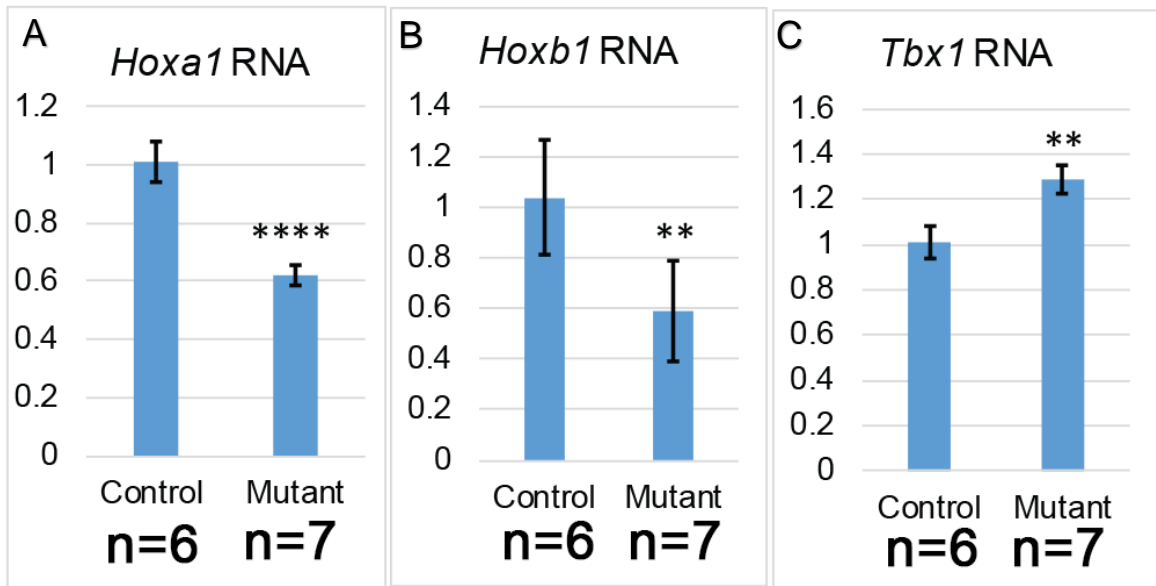


Figure 22. Expression of Pharyngeal Anterior-Posterior Patterning Genes. (A-C) Expression of pharyngeal patterning genes in cervical tissues was assessed by qPCR. Cervical tissue was isolated from E10.5 embryos by micro-dissection. In *Rdh10^{delta/flox}* mutant embryos *Hoxa1* and *Hoxb1* is reduced to 60% that of control embryos (A, B), while *Tbx1* is increased to 130% relative to control embryos (C). All gene expression differences, $p \leq 0.01$ based off Student T-Test.

These data, demonstrating reduced pharyngeal RA signaling and altered expression of key pharyngeal patterning genes, suggest a molecular mechanism for the pharyngeal skeletal and motor nerve defects observed in *Rdh10^{delta/flox}* mutant embryos.

3.8 In Utero Spontaneous Mouth Movement is Restricted in *Rdh10^{delta/flox}* Mutant Embryos

The combined evidence of the disrupted tongue morphology, the mis-patterned motor nerves, and abnormal development of the pharyngeal skeleton, led us to hypothesize that retinoid deficient embryos have a problem with mouth and tongue movement *in utero*. Vertebrate embryos begin spontaneous neuromuscular movement of the mandible and tongue before birth (Walker, 1969; Wragg et al., 1972). In mouse, these movements begin at E14.5. To determine if retinoid deficient embryos have a defect in spontaneous mandible/tongue movement, we evaluated embryo movement *in utero* via ultrasound (Fig. 23, Fig. 24). In order to have certainty regarding the genotype of embryos analyzed *in utero*, the ultrasound experiments were performed on pregnant dams crossed homozygous such that every embryo of the litter was either *Rdh10^{flox/flox}* mutant, or every embryo was *Rdh10^{+/+}* control. In each case tamoxifen was administered at E8.5, consistent with all previous experiments in this study.

Ultrasound analysis was performed on E14.5 *Rdh10^{+/+}* control and *Rdh10^{flox/flox}* mutant embryos *in utero*. For each pregnant dam, a single embryo, oriented with

a sagittal profile suitable for viewing, was analyzed for a 20 minute period. In both control and mutant embryos, periodic spontaneous movements were observed. In both groups, the head would jerk quickly back away from the abdominal cavity creating space for the mandible to depress. In control embryos each head movement was accompanied by opening of the mandible and a retraction of the tongue (Fig. 23 A) (See movie 1).

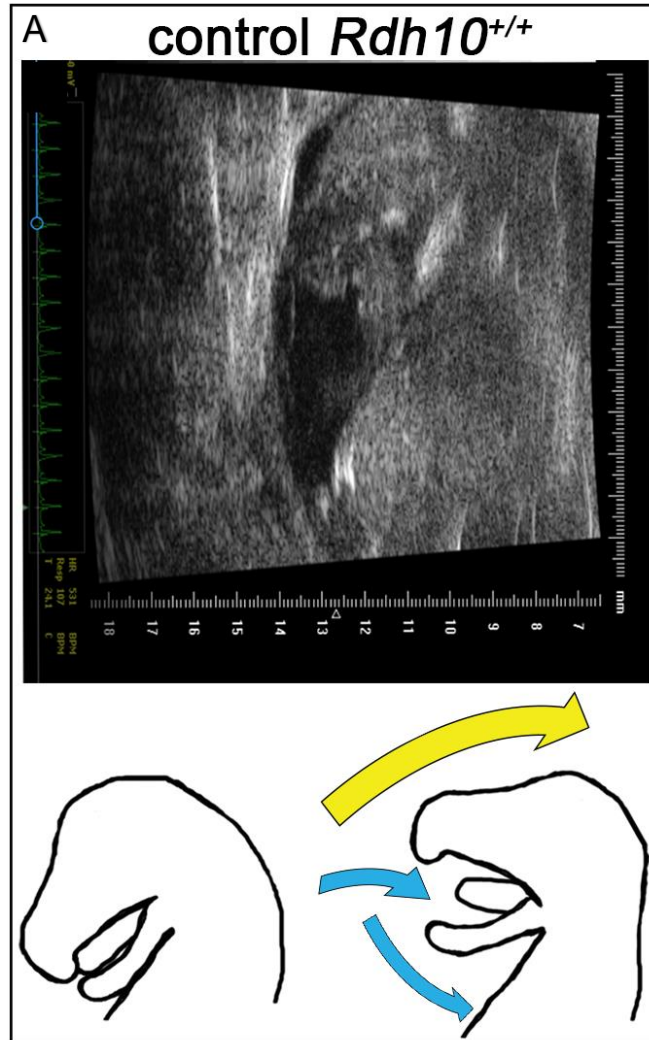


Figure 23. Control Ultrasound Still and Movement Schematic. Ultrasound analysis reveals that spontaneous mouth movement is restricted in *Rdh10^{delta/flox}* mutant embryos. Ultrasound was performed on E15.5 embryos *in utero* to evaluate spontaneous fetal mouth movement. Spontaneous movement of the head was detected in both control and mutant embryos, but mouth opening and tongue withdrawal was only observed in control embryos. (A) Still image from an ultrasound of an *Rdh10^{+/+}* control embryo. Schematic drawing depicts movement observed in control embryos. Each movement event in control embryos includes opening of the mandible and withdrawal of tongue (blue arrows), simultaneous with backwards extension of the head (yellow arrow) (see movie 1)

In contrast, in mutant embryos, the backward head extension movement was not accompanied by mouth opening. Instead, the jaw remained closed and tongue appeared inactive (Fig. 24 A) (See movie 2).



Figure 24. Mutant Ultrasound Still and Movement Schematic. (A) Still image from an ultrasound of an *Rdh10*^{flox/flox} mutant embryo. Schematic drawing depicts movement observed *Rdh10*^{flox/flox} mutant embryos. Mutant embryo movement is limited to backwards extension of the head (yellow arrow). Mandible opening and tongue withdrawal are not observed in mutant embryos (see movie 2).

In control embryos, backwards head extension with accompanying mandible/tongue movement was observed with an average frequency of 7 openings per 20 minute observation interval (Fig. 25 A, B). Mutant embryos exhibited backward head extension only without mandible/tongue movement, at an average frequency of 2.5 openings per 20-minute observation interval (Fig. 25 A, B). For one mutant embryo, spontaneous head movement was not detected, although the embryo did have a viable heartbeat.

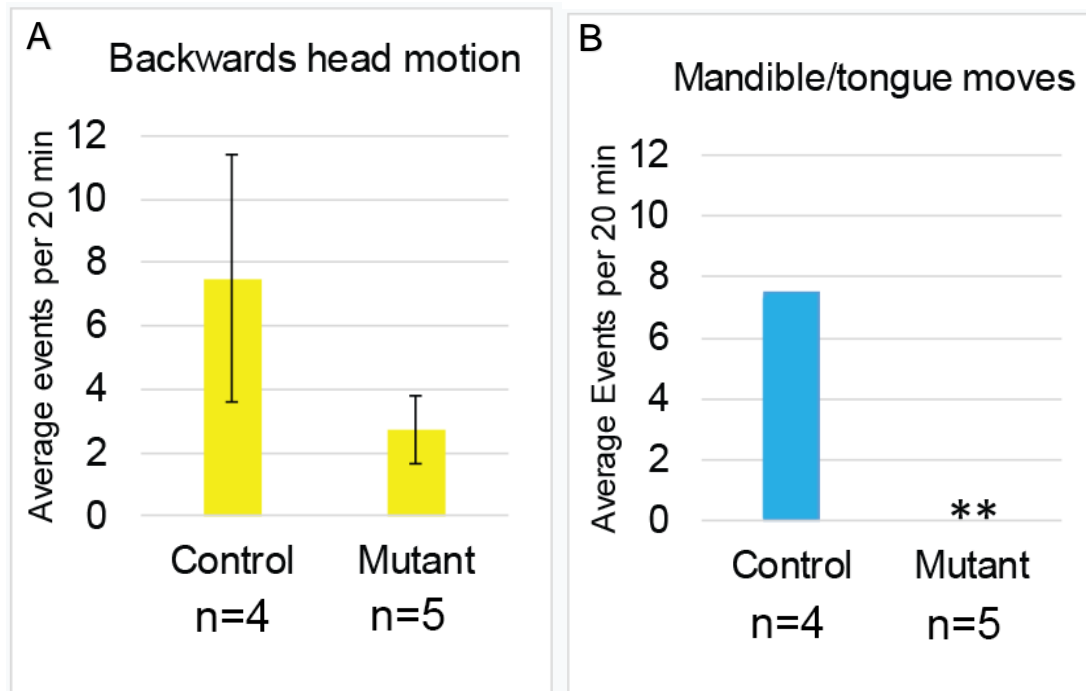


Figure 25. Statistical Comparison of Ultrasound Movements. Both control and mutant embryos exhibited backwards head motion with an average frequency of 2.5 – 7 movements per 20 minute observation interval. The frequency of head movement was not significantly different between control and mutant embryos. (A) Control embryos exhibited mouth opening and tongue withdrawal with each head movement (average frequency 7 openings per 20 minute observation interval). (B) No mouth opening or tongue withdrawal was observed in mutant embryos. The difference in frequency of mouth opening was significantly different between control and mutant embryos using Fischer’s Exact Test for independence $p \leq 0.01$.

These data demonstrate that *Rdh10* and RA signaling are not essential for spontaneous fetal backward head extension, but are necessary for functional opening of the mandible and withdrawal of the tongue.

CHAPTER 4: DISCUSSION

4.1 Identifying the Role of Retinoic Acid in Palate Development

The results from this study have identified the mechanism of cleft palate in retinoid deficiency, thus identifying the requirement of endogenous RA signaling in palate formation during embryonic development. This study documents that known patterning defects, specific to the caudal pharyngeal arch and arising from aberrant RA signaling in the posterior pharyngeal arch endoderm, result in many abnormalities to the pharyngeal arch derived elements. These defective pharyngeal arch derivatives affect a critical mechanical mechanism that is important for palate formation. During retinoid deficiency, morphology of the pharyngeal skeleton and nerves are disrupted, resulting in lack of spontaneous mouth movement at stage E14.5 in mouse.

The well reported role of RA signaling function in hind brain and neural crest patterning lends itself to the explanation of defects observed in this study. RA is known to regulate expression of the *Hox* gene family members. These genes pattern the anterior-posterior axis and body plan of the embryo. Lack of RA signaling in the model we describe, gives rise to gene expression changes in *Hox* genes. This disruption in gene expression that arises from aberrant RA signaling

likely gives rise to defects in hindbrain patterning which may well contribute to the neural and cartilage defects observed within this study.

Using an *Rdh10*^{delta/flox} mutant mouse model, this study demonstrates that endogenous RA is required for spontaneous mouth movement which is a prerequisite to elevation of the palate shelves and that this movement is only possible through proper development of pharyngeal arches. Lack of proper arch development results in vertically oriented palate shelves with the tongue residing between the shelves and obstructing their elevation.

We propose a new model linking RA signaling to palatogenesis via regulation of anterior-posterior patterning, which is crucial for formation of the neuro-structural anatomy of the pharyngeal region. The peripheral motor nerves, CN XII and C1, and the pharyngeal skeleton, including the hyoid bone, the thyroid and cricoid cartilages, work synergistically to anchor and move the muscles of the tongue and mandible (Fig. 26).

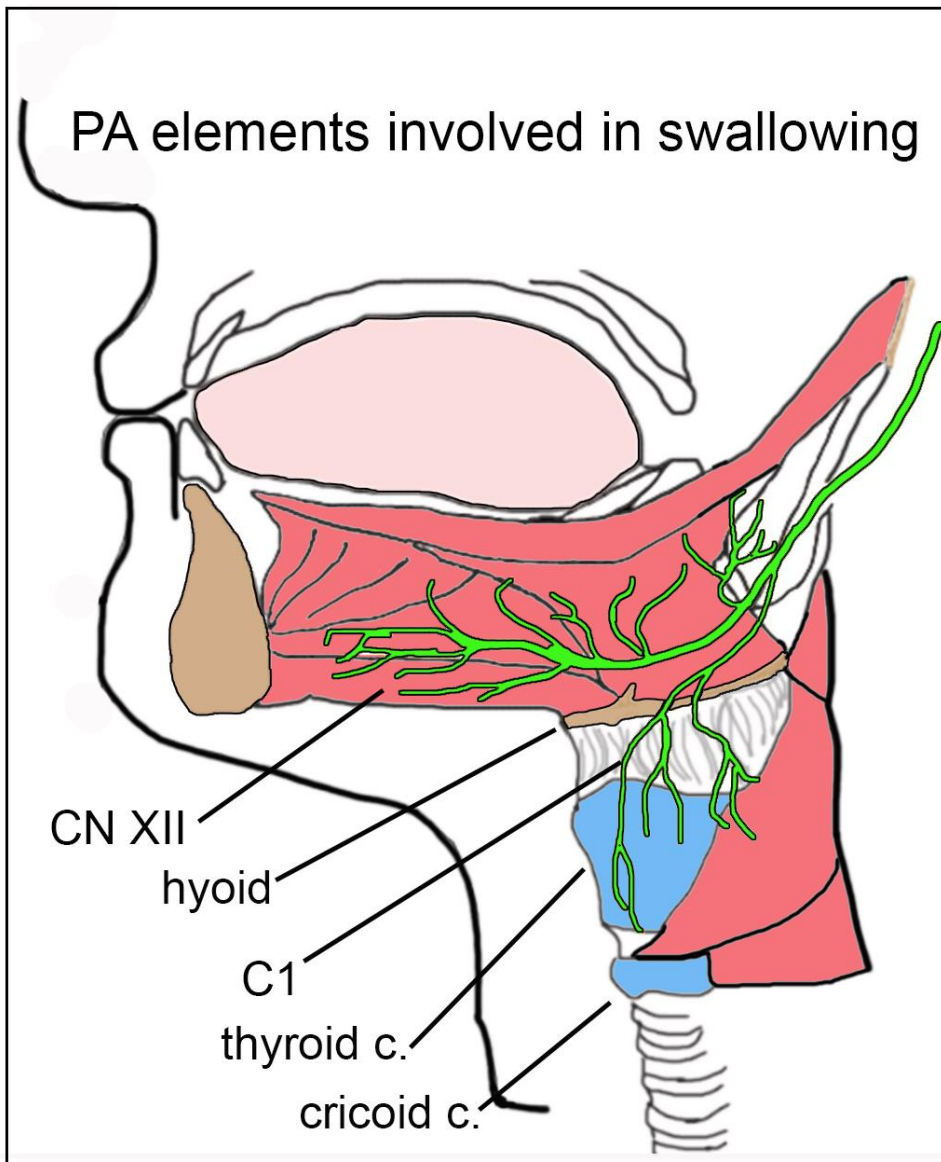


Figure 26. Schematic Drawing of the Pharyngeal Arch Elements that are Involved in Swallowing. Motor nerves and cartilages that allow mandible and tongue movement must be properly patterned via RA signaling to enable palate closure during embryogenesis. Elements of the pharyngeal arches involved in mouth movement and swallowing include the hyoid bone, the thyroid and cricoid cartilages, CN XII and C1, and muscles that attach the tongue and mandible to the pharyngeal skeleton.

Mouth opening and tongue withdrawal begins simultaneously with palate elevation during embryogenesis (Walker, 1969). At this time CN XII establishes connection to the tongue and initiates motor nerve activity (Wragg et al., 1972). This initiation of tongue movement prepares the embryo for swallowing, and also functions to make room for palate shelf elevation. This study links RDH10-mediated metabolism of vitamin A and RA regulation of genes which pattern the anterior-posterior axis of the embryo, to an anatomical mechanism of spontaneous fetal mouth movement which is critical for palate shelf elevation (Fig. 27).

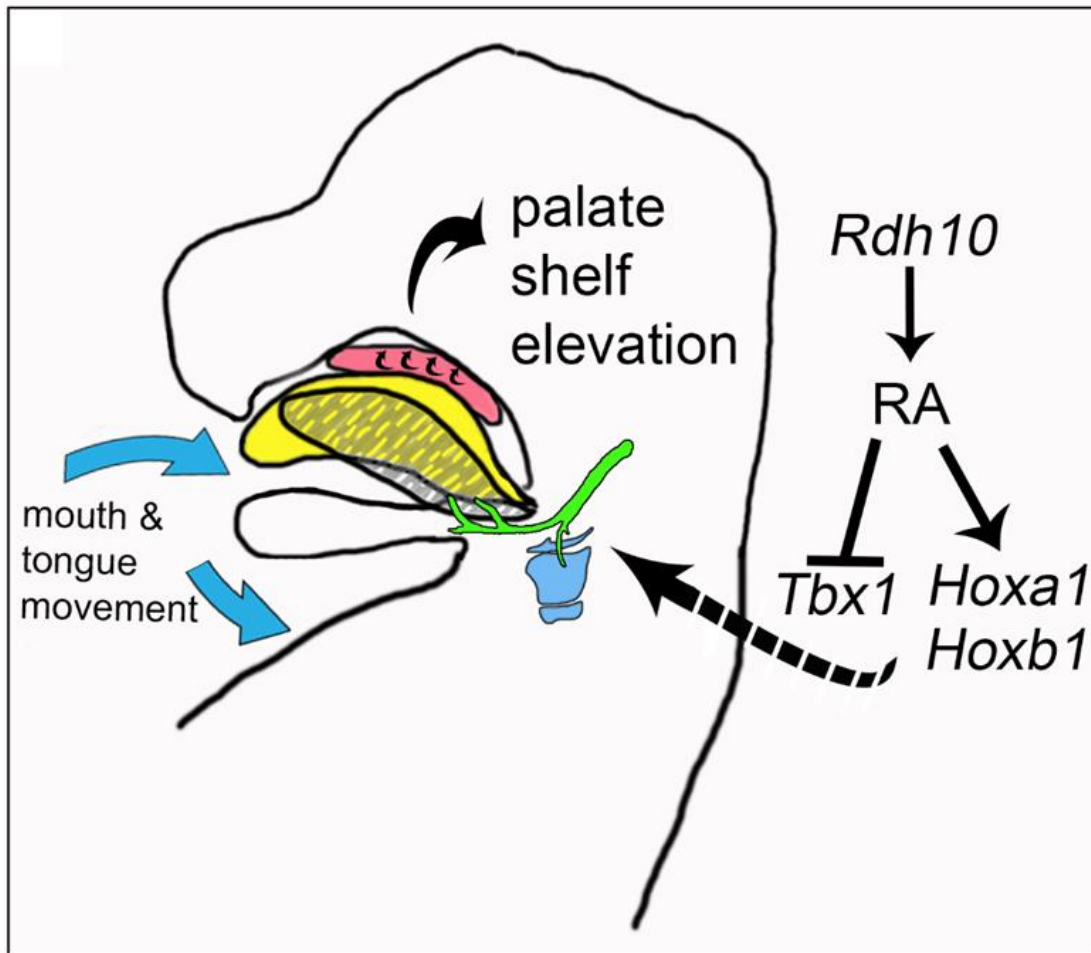


Figure 27. Schematic Drawing of Proposed Mechanism for the Role of Vitamin A and RA in Palate Formation. During embryogenesis, RA signaling, which depends on *Rdh10*-mediated retinol metabolism, is essential for proper regulation of pharyngeal patterning genes, including *Tbx1*, *Hoxa1* and *Hoxb1*. These genes are critical for patterning the anterior-posterior axis during embryonic development. The patterning of the pharyngeal region allows for proper development of the motor nerves, cartilage and muscle attachments that enable spontaneous fetal mouth movement. This movement allows the resting tongue (yellow) to depress and retract (hatched grey). The retraction moves the tongue out of the way of the palate shelves, giving them room to elevate and fuse to close the dome of the oral cavity.

Tongue interference with palate shelf closure has been suggested in previous mouse models of cleft palate. Increased tongue height has been posited to play a role in inhibiting the palate shelves from elevating (Song et al., 2013). The microCT analysis of retinoid deficient embryos presented here sheds a new light on the 3D morphology of the tongue in the context of obstructing palate shelf elevation. In mutant embryos, tongues are statistically smaller by volume, but have a heightened posterior aspect. The 3D rendering reveals that a heightened appearance could be the result of posterior tongue contraction caused by a defect in neuro-structural ability of the embryo to depress the tongue. These observations suggest that interpretation of tongue height from 2D histological sections should be made with caution.

4.2 Novel Identification of Fetal Mouth Immobility

To date, there are three categories to which the etiology of cleft palate is classified under: 1) Defect intrinsic to the palate shelf tissues, 2) defect extrinsic to the palate tissues such as reduced size of the mandible, 3) defective *in utero* spontaneous mouth movement. However, there has only been one experimental, direct demonstration of defective spontaneous mouth movement leading to cleft palate, which concludes that neurotransmitter defects are the cause. Contrary to many popular models of secondary cleft palate, this study determines that the cause of cleft palate in retinoid deficiency is not due to an intrinsic defect, nor is it due to a micrognathic mandible.

It has been postulated since the early 20th century that fetal mouth movement plays an intimate role with formation of the secondary palate (His, 1901).

Defects in spontaneous fetal mouth movement as a cause of cleft palate have been previously documented (Tsunekawa et al., 2005; Walker, 1969). However, mouth immobility as a cause of cleft palate has been shown in terms of defects in neurotransmission. Although a few additional studies infer that lack of mouth movement impacts palate formation, sufficient documentation depicting lack of *in utero* mouth movement is lacking.

This study expands the scope of defects that can disrupt spontaneous mouth movement and shows a direct demonstration of mouth immobility leading to cleft palate. Anterior-posterior patterning function of RA is needed for proper formation of the nerves and skeletal elements that enable fetal mouth movement, without which, lead to fetal mouth immobility and cleft palate. The finding that pharyngeal defects can be a cause of cleft palate by restricting fetal mouth movement identifies the previously unknown etiology and describes the requirement for endogenous RA signaling during embryonic development.

4.3 Cleft Palate in *Rdh10^{delta/flox}* Mutant Embryos is likely caused by a Combination of Defects in Nerve Routing and Muscle Attachment

Pediatric Dysphagia is a human condition that inhibits such processes as feeding and swallowing in early post-natal life. This disorder is a key phenotype of DiGeorge Syndrome. Two mouse mutant models which recapitulate DiGeorge Syndrome are the *LgDel* mutant model and the *Tbx1* mutant model (LaMantia et

al., 2016; Wang et al., 2017). It has been demonstrated that both the *LgDel* model and the *Tbx1* mutant model exhibit hyoid defects. However, the *LgDel* model of 22q11.2 deletion syndrome also possessed hypoglossal neurotransmitter defects which were correlated to feeding and swallowing difficulties during the neonatal period. These more severe nerve defects were not observed in the *Tbx1* model for 22q11.2 deletion syndrome. The conclusions of these studies emphasize the importance of proper function of the nerves that innervate muscles involved in feeding and swallowing as well as show that loss of nerve function can be a sole cause swallowing difficulties in early post-natal life. (Wang et al., 2017).

The development of muscles involved in swallowing and anchoring structures supporting them, is required for initiation of swallowing and development of the secondary palate. Mutant mouse lines for *Hoxa2* and *Hoxa1* demonstrate that disruptions in these patterning genes produce phenotypes in the origin/insertion of the extrinsic tongue musculature. These defects in the extrinsic tongue muscles are directly correlated to cleft palate concluding that tongue immobility is the cause of cleft palate in these mutant specimens. The conclusions of this study emphasize the importance of proper patterning of the extrinsic tongue musculature and show that defects in muscle morphogenesis are the sole cause of cleft palate. This study does not conclude that nerve defects are the cause of cleft palate in *Hoxa2* mutants (Barrow & Capecchi, 1999).

We infer from these two separate models, that in *Rdh10^{delta/flox}* mutant embryos, either defects in function of the hypoglossal nerve or in the attachment of the

tongue muscles to the dysplastic pharyngeal cartilage can cause cleft palate shown by defective spontaneous fetal mouth movement. Here we directly demonstrate for the first time that spontaneous fetal mouth movement is inhibited in RDH10 mutants, likely owing to a combination of aberrant nerve patterning and extrinsic tongue muscle morphogenesis. We reach this conclusion by showing abnormalities in the pharyngeal skeleton as well as patterning of nerves which control swallowing function.

Previous studies documenting mouth immobility as a cause of cleft palate utilized mutations that disrupt neurotransmitter signaling (Asada et al., 1997; Condie et al., 1997; Culiati et al., 1995; Homanics et al., 1997; Wojcik et al., 2006).

Neurotransmitter defects associated with cleft palate can originate specifically in the central nervous system (Oh et al., 2010), and can be traced to a lack of spontaneous fetal mouth movement (Tsunekawa et al., 2005). The lack of mouth movement we describe here parallels that observed in the neurotransmitter models. However, in the retinoid deficient embryos, the defect in mouth movement results from mis-patterning of peripheral motor nerves rather than a loss of neurotransmitter function. Moreover, the mouth movement defect described here was isolated to the mandible and tongue, while backwards head extension remained active.

4.4 RA Deficiency Etiology in Cleft Palate Make Have Implications in Other Contexts

In human cleft palate patients and mouse models, pharyngeal defects have been observed in association with cleft palate. Abnormalities in location and formation of the hyoid bone have been observed in human cleft palate populations (Rajion et al., 2006; Wahaj, Gul e, & Ahmed, 2014). 22q11.2 deletion syndrome in human patients includes pediatric dysphagia and defects in development of the pharyngeal arches, heart, and palate (Scambler, 2010). Defects in cranial nerve patterning and neurotransmission have been noted in mouse models of 22q11.2 deletion syndrome (Karpinski et al., 2014; Wang et al., 2017). We hypothesize that, in some cases, these pharyngeal defects may be a causal factor in the etiology of cleft palate.

The major cause of 22q11.2 deletion syndrome is loss of *Tbx1*, which is inversely regulated by RA signaling (Merscher et al., 2001; Roberts, Ivins, James, & Scambler, 2005; Scambler, 2010; Yutzey, 2010). A link between 22q11.2 deletion syndrome and perturbation of RA signaling has been well established (Yutzey, 2010). Mouse models with disrupted RA signaling have phenotypes reminiscent of 22q11.2 deletion syndrome (K. Niederreither et al., 2003; Vermot et al., 2003). Excess RA downregulates *Tbx1* expression, while reduced RA results in overexpression of *Tbx1* (Roberts et al., 2005; Ryckebusch et al., 2010). Because pharyngeal arch development depends on a precise balance between *Tbx1* and RA, we suspect that the cause of cleft palate in 22q11.2 deletion syndrome may be related to pharyngeal patterning defects similar to those we

observe in the retinoid deficient *Rdh10^{flox/delta}* mutant embryos. Perhaps correlation of cleft palate and pharyngeal arch defects in other models like 22q11.2 deletion syndrome can be understood through evaluating the presence of spontaneous mouth movement *in utero*.

CHAPTER 5: CONCLUSIONS

The data presented in our study show that RA is critical for palate development, not for a role within the palate shelf primordia, but rather its well established role in the formation of pharyngeal elements responsible for moving the mouth and tongue. This is demonstrated by lack of movement at E14.5 and defects in morphology of the peripheral motor nerves, cartilage, muscle attachment and position of the tongue in retinoid deficient embryos. This study, may be applicable to cleft palate etiology in humans. Although there are structural differences between mouse and human palate shelves during development (Yu, Deng, Nalwai-Cecchini, Glass, & Cox, 2017), it seems plausible that insufficient fetal tongue movement could obstruct palate shelf elevation in humans as it does in mice. Further investigation of this mechanism is important as it may have ramifications for preventing birth defects. More attention must be given to the optimization of RA levels during pregnancy as counseling objectives may be improved through modulation of this dynamic and sensitive signaling pathway.

REFERENCES

- Abashev, T. M., Metzler, M. A., Wright, D. M., & Sandell, L. L. (2017). Retinoic acid signaling regulates Krt5 and Krt14 independently of stem cell markers in submandibular salivary gland epithelium. *Dev Dyn*, 246(2), 135-147. doi:10.1002/dvdy.24476
- Asada, H., Kawamura, Y., Maruyama, K., Kume, H., Ding, R. G., Kanbara, N., . . . Obata, K. (1997). Cleft palate and decreased brain gamma-aminobutyric acid in mice lacking the 67-kDa isoform of glutamic acid decarboxylase. *Proc Natl Acad Sci U S A*, 94(12), 6496-6499.
- Barrow, J. R., & Capecchi, M. R. (1999). Compensatory defects associated with mutations in Hoxa1 restore normal palatogenesis to Hoxa2 mutants. *Development*, 126(22), 5011-5026.
- Bel-Vialar, S., Itasaki, N., & Krumlauf, R. (2002). Initiating Hox gene expression: in the early chick neural tube differential sensitivity to FGF and RA signaling subdivides the HoxB genes in two distinct groups. *Development*, 129, 5103-5115.
- Burdi, A. R., & Faist, K. (1967). Morphogenesis of the palate in normal human embryos with special emphasis on the mechanisms involved. *American Journal of Anatomy*, 120(1), 149-159. doi:10.1002/aja.1001200112
- Bush, J. O., & Jiang, R. (2012). Palatogenesis: morphogenetic and molecular mechanisms of secondary palate development. *Development*, 139(2), 231-243. doi:10.1242/dev.067082
- Chojnowski, J. L., Trau, H. A., Masuda, K., & Manley, N. R. (2016). Temporal and spatial requirements for Hoxa3 in mouse embryonic development. *Dev Biol*, 415(1), 33-45. doi:10.1016/j.ydbio.2016.05.010
- Condie, B. G., Bain, G., Gottlieb, D. I., & Capecchi, M. R. (1997). Cleft palate in mice with a targeted mutation in the gamma-aminobutyric acid-producing enzyme glutamic acid decarboxylase 67. *Proc Natl Acad Sci U S A*, 94(21), 11451-11455.

- Culiat, C. T., Stubbs, L. J., Woychik, R. P., Russell, L. B., Johnson, D. K., & Rinchik, E. M. (1995). Deficiency of the beta 3 subunit of the type A gamma-aminobutyric acid receptor causes cleft palate in mice. *Nat Genet*, *11*(3), 344-346. doi:10.1038/ng1195-344
- Cunningham, T. J., & Duester, G. (2015). Mechanisms of retinoic acid signalling and its roles in organ and limb development. *Nat Rev Mol Cell Biol*, *16*(2), 110-123. doi:10.1038/nrm3932
- de Vries, J. I., Visser, G. H., & Prectl, H. F. (1985). The emergence of fetal behaviour. II. Quantitative aspects. *Early Hum Dev*, *12*(2), 99-120.
- Deschamps, J., & van Nes, J. (2005). Developmental regulation of the Hox genes during axial morphogenesis in the mouse. *Development*, *132*(13), 2931-2942. doi:10.1242/dev.01897
- Diez del Corral, R., & Storey, K. G. (2004). Opposing FGF and retinoid pathways: a signalling switch that controls differentiation and patterning onset in the extending vertebrate body axis. *Bioessays*, *26*, 857-869.
- Duester, G. (2008). Retinoic acid synthesis and signaling during early organogenesis. *Cell*, *134*(6), 921-931. doi:10.1016/j.cell.2008.09.002
- Gavalas, A., Studer, M., Lumsden, A., Rijli, F. M., Krumlauf, R., & Chambon, P. (1998). Hoxa1 and Hoxb1 synergize in patterning the hindbrain, cranial nerves and second pharyngeal arch. *Development*, *125*(6), 1123-1136.
- Giudice, A., Barone, S., Belhous, K., Morice, A., Soupre, V., Bennardo, F., . . . Picard, A. (2018). Pierre Robin sequence: A comprehensive narrative review of the literature over time. *J Stomatol Oral Maxillofac Surg*. doi:10.1016/j.jormas.2018.05.002
- Hale, F. (1935). The relation of vitamin A to anophthalmos in pigs. *American Journal of Ophthalmology*, *18*, 1087-1092.
- Halilagic, A., Ribes, V., Ghyselinc, N. B., Zile, M. H., Dollé, P., & Studer, M. (2007). Retinoids control anterior and dorsal properties in the developing forebrain. *Developmental Biology*, *303*(1), 362-375. doi:http://dx.doi.org/10.1016/j.ydbio.2006.11.021
- Halilagic, A., Zile, M. H., & Studer, M. (2003). A novel role for retinoids in patterning the avian forebrain during presomite stages. *Development*, *130*(10), 2039-2050.
- Hand, J. L. (2012). Retinoic acid: a familiar teratogen. *Pediatr Dermatol*, *29*(6), 774-776. doi:10.1111/j.1525-1470.2012.01790.x

- Hernandez, R. E., Putzke, A. P., Myers, J. P., Margaretha, L., & Moens, C. B. (2007). Cyp26 enzymes generate the retinoic acid response pattern necessary for hindbrain development. *Development*, 134. doi:10.1242/dev.02706
- His, W. (1901). *Beobachtungen zur geschichte der nasen und gaumenbildung beim menschlichen embryo*. Leipzig: B. G. Teubner.
- Homanics, G. E., DeLorey, T. M., Firestone, L. L., Quinlan, J. J., Handforth, A., Harrison, N. L., . . . Olsen, R. W. (1997). Mice devoid of gamma-aminobutyrate type A receptor beta3 subunit have epilepsy, cleft palate, and hypersensitive behavior. *Proc Natl Acad Sci U S A*, 94(8), 4143-4148.
- Hu, X., Gao, J., Liao, Y., Tang, S., & Lu, F. (2013). Retinoic acid alters the proliferation and survival of the epithelium and mesenchyme and suppresses Wnt/beta-catenin signaling in developing cleft palate. *Cell Death Dis*, 4, e898. doi:10.1038/cddis.2013.424
- Huang, H. Z., Lu, B. H., Chen, Y. Y., & Liao, G. Q. (2003). [Study on etiology of retinoic acid-induced cleft palate in mouse]. *Zhonghua Kou Qiang Yi Xue Za Zhi*, 38(3), 185-187.
- Jin, J. Z., Tan, M., Warner, D. R., Darling, D. S., Higashi, Y., Gridley, T., & Ding, J. (2010). Mesenchymal cell remodeling during mouse secondary palate reorientation. *Dev Dyn*, 239(7), 2110-2117. doi:10.1002/dvdy.22339
- Karpinski, B. A., Maynard, T. M., Fralish, M. S., Nuwayhid, S., Zohn, I. E., Moody, S. A., & LaMantia, A. S. (2014). Dysphagia and disrupted cranial nerve development in a mouse model of DiGeorge (22q11) deletion syndrome. *Dis Model Mech*, 7(2), 245-257. doi:10.1242/dmm.012484
- Kurosaka, H., Wang, Q., Sandell, L., Yamashiro, T., & Trainor, P. A. (2017). Rdh10 loss-of-function and perturbed retinoid signaling underlies the etiology of choanal atresia. *Hum Mol Genet*. doi:10.1093/hmg/ddx031
- LaMantia, A. S., Moody, S. A., Maynard, T. M., Karpinski, B. A., Zohn, I. E., Mendelowitz, D., . . . Popratiloff, A. (2016). Hard to swallow: Developmental biological insights into pediatric dysphagia. *Dev Biol*, 409(2), 329-342. doi:10.1016/j.ydbio.2015.09.024
- Lan, Y., Zhang, N., Liu, H., Xu, J., & Jiang, R. (2016). Golgb1 regulates protein glycosylation and is crucial for mammalian palate development. *Development*, 143(13), 2344-2355. doi:10.1242/dev.134577

- Livak, K. J., & Schmittgen, T. D. (2001). Analysis of relative gene expression data using real-time quantitative PCR and the 2^{-Delta Delta C(T)} Method. *Methods*, 25(4), 402-408. doi:10.1006/meth.2001.1262
- Lohnes, D., Mark, M., Mendelsohn, C., Dolle, P., Dierich, A., Gorry, P., . . . Chambon, P. (1994). Function of the retinoic acid receptors (RARs) during development (I). Craniofacial and skeletal abnormalities in RAR double mutants. *Development*, 120(10), 2723-2748.
- Luo, J., Sucov, H. M., Bader, J. A., Evans, R. M., & Giguere, V. (1996). Compound mutants for retinoic acid receptor (RAR) beta and RAR alpha 1 reveal developmental functions for multiple RAR beta isoforms. *Mech Dev*, 55(1), 33-44.
- Mark, M., Ghyselinck, N. B., & Chambon, P. (2004). Retinoic acid signalling in the development of branchial arches. *Curr Opin Genet Dev*, 14(5), 591-598. doi:10.1016/j.gde.2004.07.012
- McCaffery, P. J., Adams, J., Maden, M., & Rosa-Molinar, E. (2003). Too much of a good thing: retinoic acid as an endogenous regulator of neural differentiation and exogenous teratogen. *Eur J Neurosci*, 18(3), 457-472.
- McDonald-McGinn, D. M., Sullivan, K. E., Marino, B., Philip, N., Swillen, A., Vorstman, J. A. S., . . . Bassett, A. S. (2015). 22q11.2 deletion syndrome. *Nature Reviews Disease Primers*, 1, 15071. doi:10.1038/nrdp.2015.71
- Merscher, S., Funke, B., Epstein, J. A., Heyer, J., Puech, A., Lu, M. M., . . . Kucherlapati, R. (2001). TBX1 is responsible for cardiovascular defects in velo-cardio-facial/DiGeorge syndrome. *Cell*, 104(4), 619-629.
- Metzler, M. A., Raja, S., Elliott, K. H., Friedl, R. M., Tran, N. Q. H., Brugmann, S. A., . . . Sandell, L. L. (2018). Correction: RDH10-mediated retinol metabolism and RARalpha-mediated retinoic acid signaling are required for submandibular salivary gland initiation (doi: 10.1242/dev.164822). *Development*, 145(17). doi:10.1242/dev.170795
- Metzler, M. A., & Sandell, L. L. (2016). Enzymatic Metabolism of Vitamin A in Developing Vertebrate Embryos. *Nutrients*, 8(12). doi:10.3390/nu8120812
- Miller, C. K. (2009). Updates on pediatric feeding and swallowing problems. *Curr Opin Otolaryngol Head Neck Surg*, 17(3), 194-199. doi:10.1097/MOO.0b013e32832b3117
- Miller, J. L., Sonies, B. C., & Macedonia, C. (2003). Emergence of oropharyngeal, laryngeal and swallowing activity in the developing fetal

upper aerodigestive tract: an ultrasound evaluation. *Early Hum Dev*, 71(1), 61-87.

- Mulder, G. B., Manley, N., & Maggio-Price, L. (1998). Retinoic acid-induced thymic abnormalities in the mouse are associated with altered pharyngeal morphology, thymocyte maturation defects, and altered expression of Hoxa3 and Pax1. *Teratology*, 58(6), 263-275. doi:10.1002/(SICI)1096-9926(199812)58:6<263::AID-TERA8>3.0.CO;2-A
- Nelson, E. R., Levi, B., & Longaker, M. T. (2011). Commentary on role of apoptosis in retinoic Acid-induced cleft palate. *J Craniofac Surg*, 22(5), 1572-1573. doi:10.1097/SCS.0b013e31822e5ea6
- Niederreither, K., & Dolle, P. (2008). Retinoic acid in development: towards an integrated view. *Nat Rev Genet*, 9(7), 541-553. doi:10.1038/nrg2340
- Niederreither, K., Subbarayan, V., Dollé, P., & Chambon, P. (1999). Embryonic retinoic acid synthesis is essential for early mouse post-implantation development. *Nature Genetics*, 21, 444-448.
- Niederreither, K., Vermot, J., Le Roux, I., Schuhbaur, B., Chambon, P., & Dolle, P. (2003). The regional pattern of retinoic acid synthesis by RALDH2 is essential for the development of posterior pharyngeal arches and the enteric nervous system. *Development*, 130(11), 2525-2534.
- Oh, W. J., Westmoreland, J. J., Summers, R., & Condie, B. G. (2010). Cleft palate is caused by CNS dysfunction in Gad1 and Viaat knockout mice. *PLoS One*, 5(3), e9758. doi:10.1371/journal.pone.0009758
- Okano, J., Suzuki, S., & Shiota, K. (2007). Involvement of apoptotic cell death and cell cycle perturbation in retinoic acid-induced cleft palate in mice. *Toxicol Appl Pharmacol*, 221(1), 42-56. doi:10.1016/j.taap.2007.02.019
- Okano, J., Udagawa, J., & Shiota, K. (2014). Roles of retinoic acid signaling in normal and abnormal development of the palate and tongue. *Congenit Anom (Kyoto)*, 54(2), 69-76. doi:10.1111/cga.12049
- Parker, S. E., Mai, C. T., Canfield, M. A., Rickard, R., Wang, Y., Meyer, R. E., . . . for the National Birth Defects Prevention, N. (2010). Updated national birth prevalence estimates for selected birth defects in the United States, 2004–2006. *Birth Defects Research Part A: Clinical and Molecular Teratology*, 88(12), 1008-1016. doi:10.1002/bdra.20735
- Piersma, A. H., Hessel, E. V., & Staal, Y. C. (2017). Retinoic acid in developmental toxicology: Teratogen, morphogen and biomarker. *Reprod Toxicol*, 72, 53-61. doi:10.1016/j.reprotox.2017.05.014

- Rajion, Z. A., Townsend, G. C., Netherway, D. J., Anderson, P. J., Hughes, T., Shuaib, I. L., . . . David, D. J. (2006). The hyoid bone in malay infants with cleft lip and palate. *Cleft Palate Craniofac J*, *43*(5), 532-538. doi:10.1597/05-085
- Rhinn, M., & Dolle, P. (2012). Retinoic acid signalling during development. *Development*, *139*(5), 843-858. doi:10.1242/dev.065938
- Ribes, V., Wang, Z., Dolle, P., & Niederreither, K. (2006). Retinaldehyde dehydrogenase 2 (RALDH2)-mediated retinoic acid synthesis regulates early mouse embryonic forebrain development by controlling FGF and sonic hedgehog signaling. *Development*, *133*(2), 351-361. doi:10.1242/dev.02204
- Roberts, C., Ivins, S. M., James, C. T., & Scambler, P. J. (2005). Retinoic acid down-regulates Tbx1 expression in vivo and in vitro. *Dev Dyn*, *232*(4), 928-938. doi:10.1002/dvdy.20268
- Rossant, J., Zirngibl, R., Cado, D., Shago, M., & Giguere, V. (1991). Expression of a retinoic acid response element-hsplacZ transgene defines specific domains of transcriptional activity during mouse embryogenesis. *Genes Dev*, *5*(8), 1333-1344.
- Ryckebusch, L., Bertrand, N., Mesbah, K., Bajolle, F., Niederreither, K., Kelly, R. G., & Zaffran, S. (2010). Decreased levels of embryonic retinoic acid synthesis accelerate recovery from arterial growth delay in a mouse model of DiGeorge syndrome. *Circ Res*, *106*(4), 686-694. doi:10.1161/circresaha.109.205732
- Sandell, L. L., Kurosaka, H., & Trainor, P. A. (2012). Whole mount nuclear fluorescent imaging: convenient documentation of embryo morphology. *Genesis*, *50*(11), 844-850. doi:10.1002/dvg.22344
- Sandell, L. L., Lynn, M. L., Inman, K. E., McDowell, W., & Trainor, P. A. (2012). RDH10 oxidation of Vitamin A is a critical control step in synthesis of retinoic acid during mouse embryogenesis. *PLoS One*, *7*(2), e30698. doi:10.1371/journal.pone.0030698
- Sandell, L. L., Sanderson, B. W., Moiseyev, G., Johnson, T., Mushegian, A., Young, K., . . . Trainor, P. A. (2007). RDH10 is essential for synthesis of embryonic retinoic acid and is required for limb, craniofacial, and organ development. *Genes Dev*, *21*(9), 1113-1124. doi:10.1101/gad.1533407
- Scambler, P. J. (2010). 22q11 deletion syndrome: a role for TBX1 in pharyngeal and cardiovascular development. *Pediatr Cardiol*, *31*(3), 378-390. doi:10.1007/s00246-009-9613-0

- Schneider, R. A., Hu, D., Rubenstein, J. L., Maden, M., & Helms, J. A. (2001). Local retinoid signaling coordinates forebrain and facial morphogenesis by maintaining FGF8 and SHH. *Development*, *128*(14), 2755-2767.
- See, A. W. M., Kaiser, M. E., White, J. C., & Clagett-Dame, M. (2008). A nutritional model of late embryonic vitamin A deficiency produces defects in organogenesis at a high penetrance and reveals new roles for the vitamin in skeletal development. *Developmental Biology*, *316*(2), 171-190.
- Sirbu, I. O., Gresh, L., Barra, J., & Duester, G. (2005). Shifting boundaries of retinoic acid activity control hindbrain segmental gene expression. *Development*, *132*(11), 2611-2622. doi:10.1242/dev.01845
- Song, Z., Liu, C., Iwata, J., Gu, S., Suzuki, A., Sun, C., . . . Chen, Y. (2013). Mice with Tak1 deficiency in neural crest lineage exhibit cleft palate associated with abnormal tongue development. *J Biol Chem*, *288*(15), 10440-10450. doi:10.1074/jbc.M112.432286
- Sperber, G. H. (2002). Palatogenesis: closure of the secondary palate. In D. F. Wyszynski (Ed.), *Cleft Lip and Palate: From Origin to Treatment* (pp. 14-24). New York: Oxford.
- Tsunekawa, N., Arata, A., & Obata, K. (2005). Development of spontaneous mouth/tongue movement and related neural activity, and their repression in fetal mice lacking glutamate decarboxylase 67. *Eur J Neurosci*, *21*(1), 173-178. doi:10.1111/j.1460-9568.2004.03860.x
- Ventura, A., Kirsch, D. G., McLaughlin, M. E., Tuveson, D. A., Grimm, J., Lintault, L., . . . Jacks, T. (2007). Restoration of p53 function leads to tumour regression in vivo. *Nature*, *445*(7128), 661-665. doi:10.1038/nature05541
- Vermot, J., Niederreither, K., Garnier, J. M., Chambon, P., & Dolle, P. (2003). Decreased embryonic retinoic acid synthesis results in a DiGeorge syndrome phenotype in newborn mice. *Proc Natl Acad Sci U S A*, *100*(4), 1763-1768. doi:10.1073/pnas.0437920100
- Wahaj, A., Gul e, E., & Ahmed, I. (2014). Comparison of hyoid bone position among cleft lip palate and normal subjects. *J Coll Physicians Surg Pak*, *24*(10), 745-748. doi:10.2014/jcpsp.745748
- Walker, B. E. (1969). Correlation of embryonic movement with palate closure in mice. *Teratology*, *2*(3), 191-197. doi:10.1002/tera.1420020304
- Wang, X., Bryan, C., LaMantia, A. S., & Mendelowitz, D. (2017). Altered neurobiological function of brainstem hypoglossal neurons in

- DiGeorge/22q11.2 Deletion Syndrome. *Neuroscience*, 359, 1-7.
doi:10.1016/j.neuroscience.2017.06.057
- Warkany, J. (1945). The Importance of Prenatal Diet. *The Milbank Memorial Fund Quarterly*, 23(1), 66-77. doi:10.2307/3348002
- Warkany, J., Nelson, R. C., & Schraffenberger, E. (1943). Congenital malformations induced in rats by maternal nutritional deficiency: Iv. cleft palate. *American Journal of Diseases of Children*, 65(6), 882-894.
doi:10.1001/archpedi.1943.02010180058007
- Wehby, G. L., & Cassell, C. H. (2010). The impact of orofacial clefts on quality of life and healthcare use and costs. *Oral Diseases*, 16(1), 3-10.
doi:10.1111/j.1601-0825.2009.01588.x
- Wendling, O., Dennefeld, C., Chambon, P., & Mark, M. (2000). Retinoid signaling is essential for patterning the endoderm of the third and fourth pharyngeal arches. *Development*, 127(8), 1553-1562.
- White, J. C., Highland, M., Kaiser, M., & Clagett-Dame, M. (2000). Vitamin A deficiency results in the dose-dependent acquisition of anterior character and shortening of the caudal hindbrain of the rat embryo. *Dev Biol*, 220(2), 263-284. doi:10.1006/dbio.2000.9635
- White, J. C., Shankar, V. N., Highland, M., Epstein, M. L., DeLuca, H. F., & Clagett-Dame, M. (1998). Defects in embryonic hindbrain development and fetal resorption resulting from vitamin A deficiency in the rat are prevented by feeding pharmacological levels of all-trans-retinoic acid. *Proc Natl Acad Sci U S A*, 95(23), 13459-13464.
- Wilson, J. G., Roth, C. B., & Warkany, J. (1953). An analysis of the syndrome of malformations induced by maternal vitamin a deficiency. Effects of restoration of vitamin a at various times during gestation. *American Journal of Anatomy*, 92(2), 189-217. doi:10.1002/aja.1000920202
- Wojcik, S. M., Katsurabayashi, S., Guillemain, I., Friauf, E., Rosenmund, C., Brose, N., & Rhee, J. S. (2006). A shared vesicular carrier allows synaptic corelease of GABA and glycine. *Neuron*, 50(4), 575-587.
doi:10.1016/j.neuron.2006.04.016
- World Health Organization. (2007). Human Genomics in Global Health: Typical Orofacial Clefts- cumulative data by Register. Retrieved from https://www.who.int/genomics/anomalies/cumulative_data/en/

- Wragg, L. E., Smith, J. A., & Borden, C. S. (1972). Myoneural maturation and function of the foetal rat tongue at the time of secondary palate closure. *Arch Oral Biol*, 17(4), 673-682.
- Yoon, H., Chung, I. S., Seol, E. Y., Park, B. Y., & Park, H. W. (2000). Development of the lip and palate in staged human embryos and early fetuses. *Yonsei Med J*, 41(4), 477-484. doi:10.3349/ymj.2000.41.4.477
- Yu, K., Deng, M., Naluai-Cecchini, T., Glass, I. A., & Cox, T. C. (2017). Differences in Oral Structure and Tissue Interactions during Mouse vs. Human Palatogenesis: Implications for the Translation of Findings from Mice. 8(154). doi:10.3389/fphys.2017.00154
- Yutzey, K. E. (2010). DiGeorge syndrome, Tbx1, and retinoic acid signaling come full circle. *Circ Res*, 106(4), 630-632. doi:10.1161/CIRCRESAHA.109.215319
- Zhang, J., Zhou, S., Zhang, Q., Feng, S., Chen, Y., Zheng, H., . . . Chen, F. (2014). Proteomic Analysis of RBP4/Vitamin A in Children with Cleft Lip and/or Palate. *Journal of Dental Research*, 93(6), 547-552. doi:10.1177/0022034514530397

CURRICULUM VITA

NAME: Regina Mary Friedl

ADDRESS: Department of Oral Immunology and Infectious Diseases
School of Dentistry
University of Louisville
502 S. Preston St.
Louisville, KY 40206

DOB: Akron, Ohio – September 12, 1992

EDUCATION AND TRAINING:

Bachelor of Science-Biology
Walsh University
2010-2014

Masters of Science-Oral Biology
University of Louisville
School of Dentistry
2017-2019

AWARDS:

Research! Louisville
2018-1st place School of Dentistry
Basic Sciences Student Award

2018-Selected to attend the Hinman Student Research Symposium with travel award

CO-AUTHORSHIP ON PUBLICATIONS/MANUSCRIPT SUBMISSION:

Metzler, M. A., Raja, S., Elliott, K. H., Friedl, R. M., Tran, N. Q. H., Brugmann, S. A., Sandell, L. L. (2018). Correction: RDH10-mediated retinol metabolism and RAR α -mediated retinoic acid signaling are required for submandibular salivary gland initiation (doi: 10.1242/dev.164822). *Development*, 145(17). doi:10.1242/dev.170795

Under Review:

Friedl, R. M., Raja, S., Metzler, M. A., Patel, N. D., Brittan, K. R., Jones, S. P., Sandell, L. L., (2018) Spontaneous fetal mouth movement essential for palate formation depends upon retinoid-mediated patterning of pharyngeal peripheral motor nerves and skeleton (2018)

NATIONAL MEETING PRESENTATIONS:

2018-7th Annual Skin Sciences and Craniofacial Research Symposium-"Cleft Palate in Retinoic Acid Deficient Rdh10 Mutant Mice is associated with Defects in Morphogenesis of Mandible and Tongue" -Poster Presentation

2018-Research! Louisville-"Rdh10 Mutant Mice Reveal Pharyngeal Patterning Defects Underlie Cleft Palate in Retinoid Deficiency" -Poster Presentation

2018-Hinman Student Research Symposium-"Rdh10 Mutant Mice Reveal Pharyngeal Patterning Defects Underlie Cleft Palate in Retinoid Deficiency" - Poster Presentation